

CELL MECHANICS

1. Introduction - L1

2. Physical principles

- 2.1. Forces at molecular and cell level - L2
- 2.2. Thermal forces, diffusion, and chemical forces;
and Single molecule experiments – L3, L4, L5, L6

3. Mechanics of the Cytoskeleton and Mechano-transduction

- 3.1. Motor proteins - types, working principle – L8-9
- 3.2. Force generation by the cytoskeleton and cell motility – L10

4. Experimental techniques to study cell mechanics

4.1. Cellular mechanotransduction (basic principles and examples) L11

- 4.2. Optical, magnetic and acoustic tweezers L7, L12
- 4.3. Super resolution optical microscopy techniques (STED, PALM) L12

- Lab visit and experimental optical tweezers cell mechanics session at CNR IOM

Outline:

- What is mechanosignaling
- What types of forces do cells encounter ?
- Examples of mechanotransduction and experimental techniques

3.3. Cellular mechanotransduction (basic principles and examples)

Mechanotransduction refers to the processes through which cells sense and respond to mechanical stimuli by converting them to biochemical signals that elicit specific cellular responses. It leads to responses such as proliferation, differentiation, migration and apoptosis.

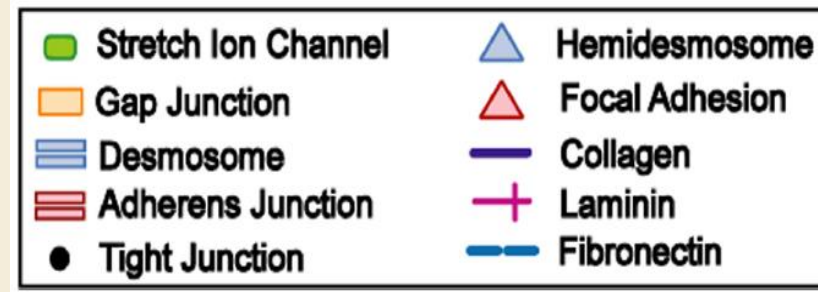
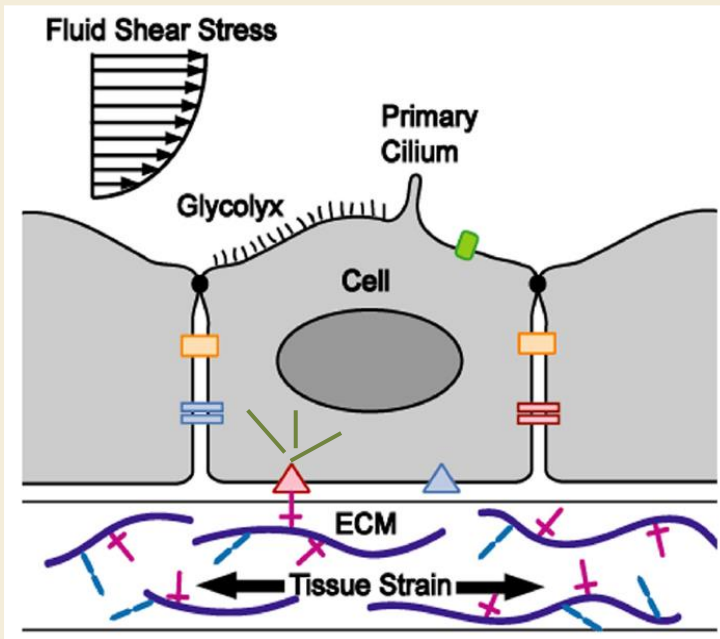
www.mechanobio.info +


Slides, examples of mechanical transduction experimental work from literature (papers)

- What is mechanosignaling ?
- What types of forces do cells encounter ?
- How are forces transduced in a cellular environment ?
- How does the cytoskeleton transmit mechanical forces ?
- How is energy transferred across the cellular system ?
- What are cell-cell adhesions ? and What are cell-matrix adhesions ?
- What are focal adhesions and how are they formed ?
- What are cell-matrix receptors?
- What is integrin and how is integrin activated ?
- Which biochemical pathways are regulated by mechanical signals ?
- How do mechanically-gated ion channels facilitate mechanotransduction ?
- What are guidance cues ?

www.mechanobio.info

What types of forces do cells encounter ?



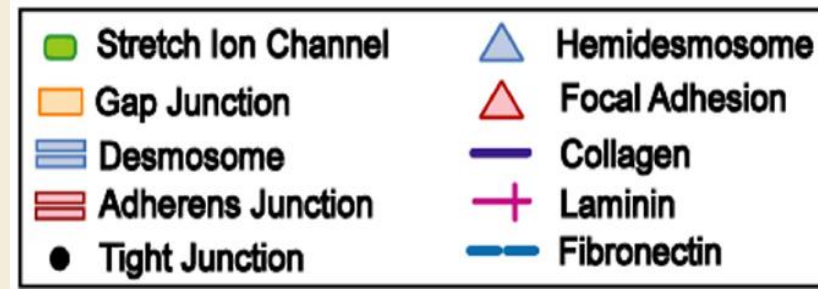
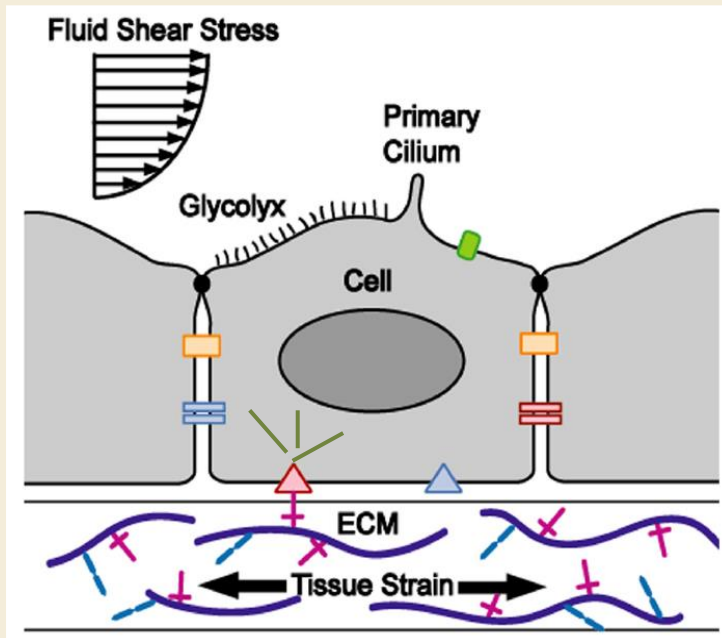
 Stress fiber

Internal forces due to the shortening of stress fibers in a cell can lead to tension at points of contact outside the cell, e.g., cell–matrix adhesions and/or cell–cell junctions.

Stress fibers are contractile actomyosin bundles found also in non-muscle cells.

ECM – extracellular matrix: a three-dimensional network of extracellular macromolecules, such as collagen, enzymes, and glycoproteins, that provide structural and biochemical support to surrounding cells

What types of forces do cells encounter ?



 Stress fiber

Tension at the cell–matrix junction acts predominately at **focal adhesions (FA)**.

FA are protein complexes at the inner surface of the cell membrane, that have both a structural and mechano signaling role.

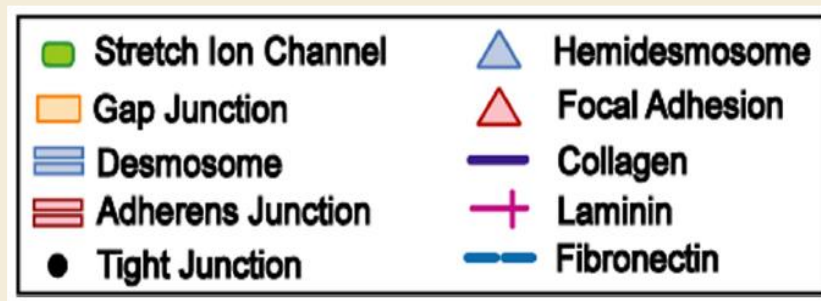
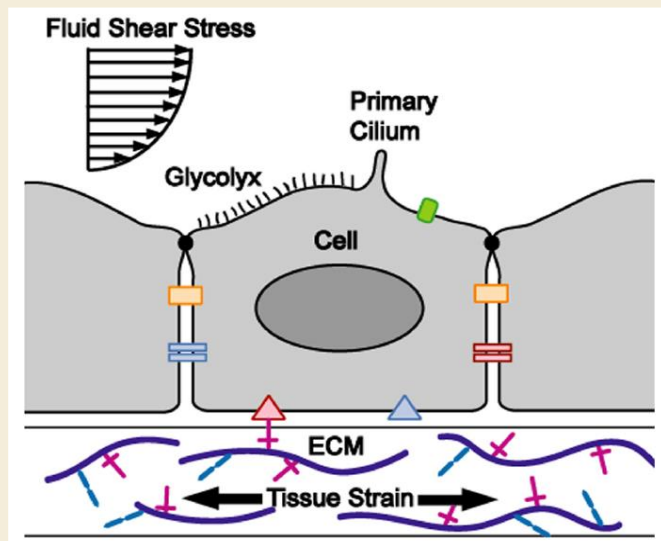
FA proteins, like **vinculin** or **talin**, connect to transmembrane receptors known as **integrins**, which subsequently connect to ligands in the **ECM**.

The forces produced by myosin can be transmitted through FA to the integrin-ECM interface, where they act as traction forces.

The spatial and temporal coordination of a cell's traction forces enable it to migrate, e.g. during wound healing.

Traction forces also provide a prestress against the ECM that regulates cell adhesion and signaling pathways associated with FAs.

What types of forces do cells encounter ?



In addition to forces created and sensed internally, cells also experience **external forces** acting on them.

They can either be **directly applied** to the cell or transmitted to the cell via cell–ECM or cell–cell **interfaces**.

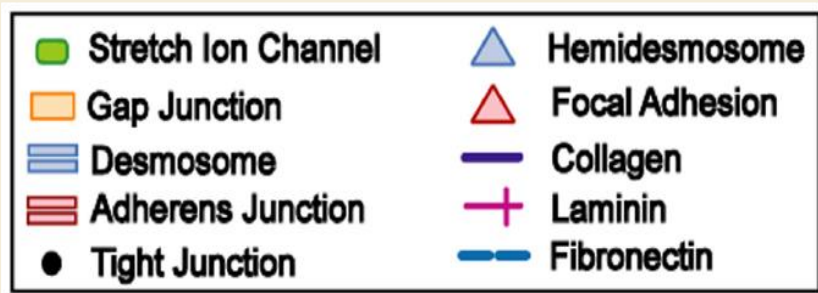
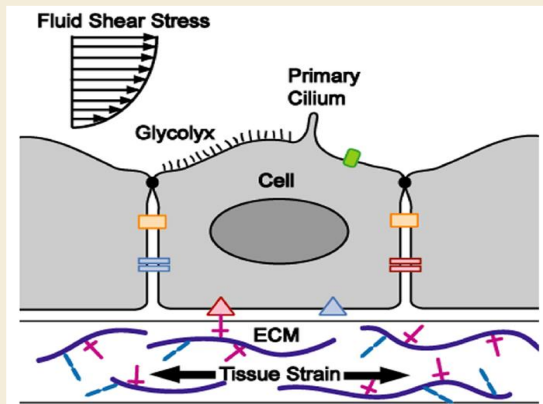
They are **sensed** by the **same mechanosensory** structures that detect internal forces but they can also be sensed by structures like the **glycocalyx**, **primary cilium**, and **stretch ion channels**.

The **glycocalyx** is a lattice of semiflexible macromolecules that are anchored in the cell membrane and extend into the extracellular environment.

Primary cilia are long, slender protrusions of the cell membrane that contain microtubules. Both the glycocalyx and primary cilia deflect much like a cantilever beam when subject to fluid flow.

Stretch ion channels, or mechanical gated ion channels, are protein complexes in the cell membrane that open their central pore in response to externally applied strains. E.g. Forces applied to the cell membrane lead to an increase in membrane tension, which then opens the channels and increases the conductance of extracellular ions that activate signaling pathways that affect cell function and gene regulation.

What are cell-cell adhesions?

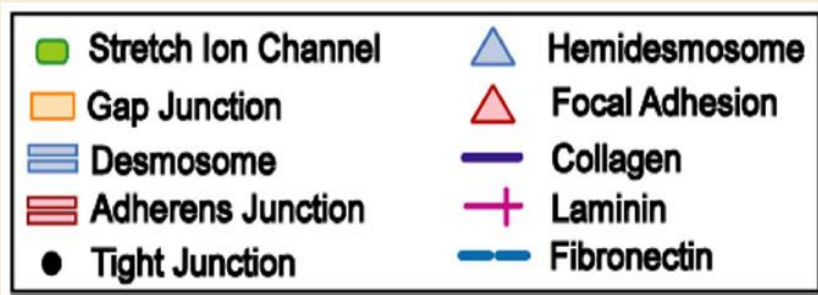
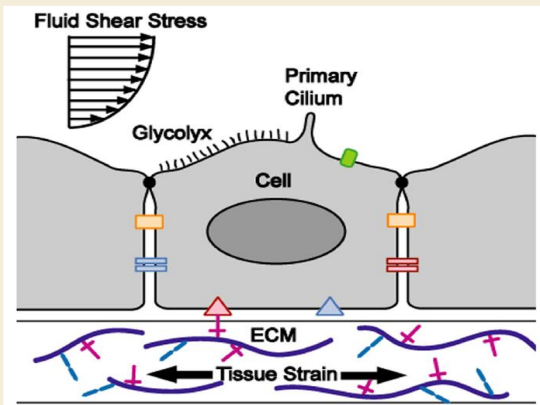


At **cell-cell junctions**, tension from actin and myosin in one cell can be transmitted to a neighboring cell.

Cell-cell junction: family of physical adhesive molecules that intracellularly connect two cells. These interactions facilitate cell-to-cell adhesion, and are also a conduit for chemical, mechanical, or electrical information between cells.

Types of cell-cell junctions: **tight junctions**, **gap junctions**, and **anchoring junctions**.

What are cell-cell adhesions?



Tight junctions are composed of proteins—occludin, claudin, and other junction adhesion molecules—which serve to form a seal between neighboring cells, and act as a physical barrier to solute diffusion between those cells.

Gap junctions are essentially pores composed of connexins, innexins, and pannexins, which allow for the transport of small molecules between adjacent cells.

Anchoring junctions : adherens junctions, desmosomes, and hemidesmosomes.

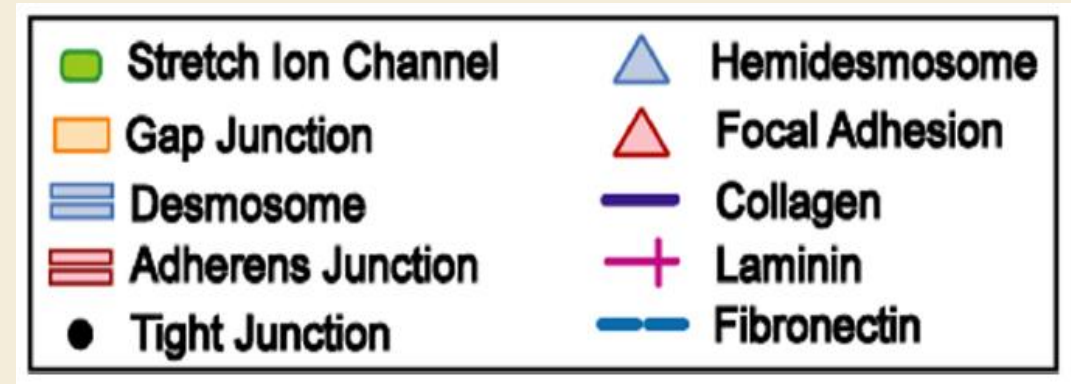
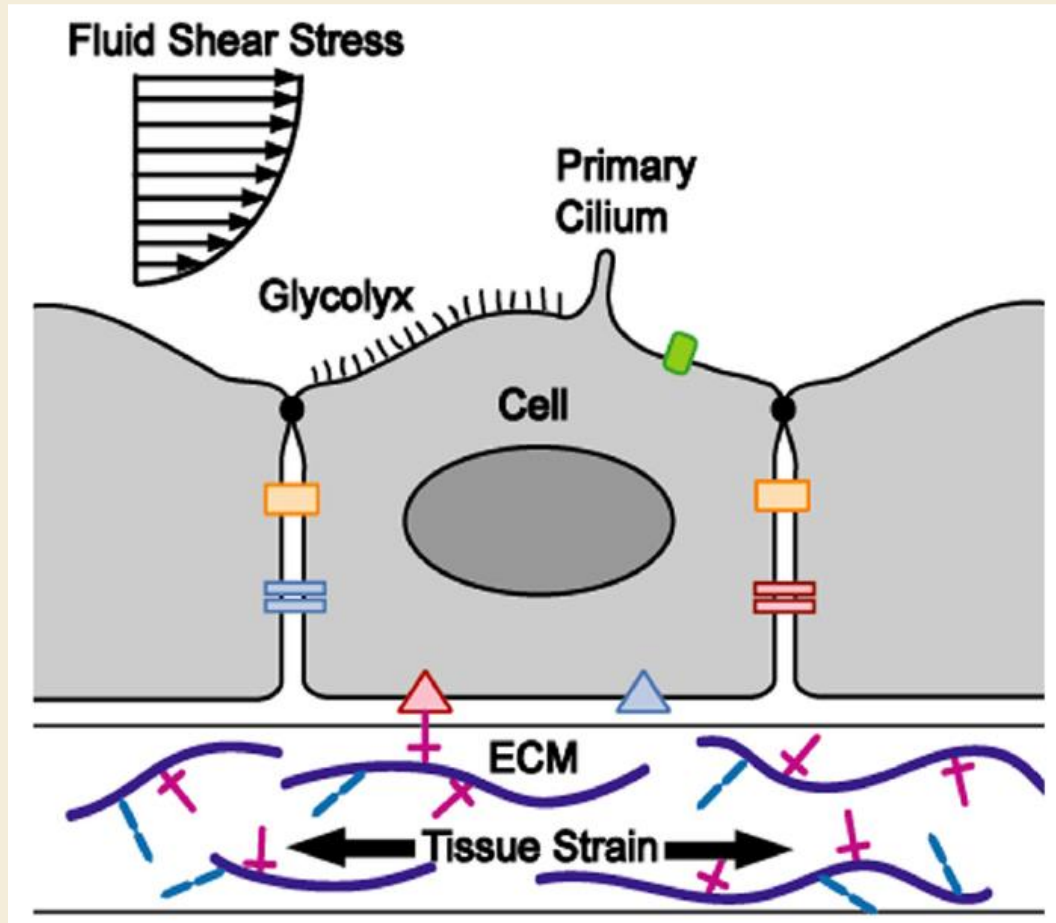
Anchoring junctions have a structural role, by maintaining cell integrity through cytoskeletal connections to other cells, as well as the ECM.

Adherens junctions connect the actin filaments of neighboring cells through cadherin proteins.

Desmosomes join cellular intermediate filaments through desmosomal cadherins.

Hemidesmosomes link a cell's intermediate filaments to the extracellular matrix through integrins.

Mechanotransduction pathways and force-sensing structures at cell–cell and cell–ECM junctions



ECM = extracellular matrix

- What is mechanosignaling ?
- What types of forces do cells encounter ?
- How are forces transduced in a cellular environment ?
- How does the cytoskeleton transmit mechanical forces ?
- How is energy transferred across the cellular system ?
- What are cell-cell adhesions ? and What are cell-matrix adhesions ?
- What are focal adhesions and how are they formed ?
- What are cell-matrix receptors?
- What is integrin and how is integrin activated ?
- Which biochemical pathways are regulated by mechanical signals ?
- How do mechanically-gated ion channels facilitate mechanotransduction ?
- What are guidance cues ?

www.mechanobio.info

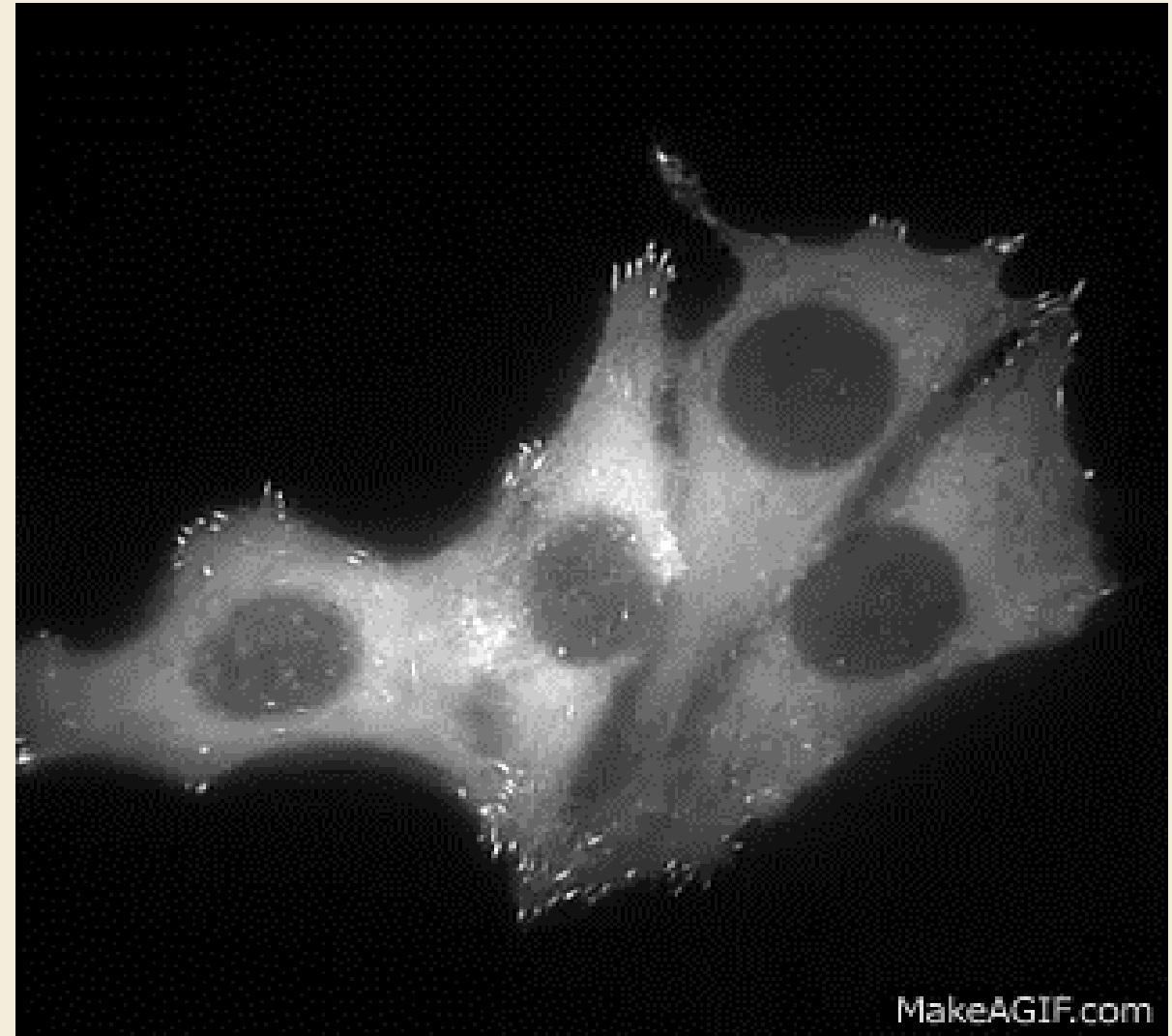
Video. **Focal adhesions** formation during lamellipodial protrusion helps cell spreading.

During lamellipodial protrusion, numerous Focals form along the cell periphery and can be visualized as fluorescent spots (GFP-VASP).

GFP – Green Fluorescence Protein

VASP – Vasodilator stimulated phosphoprotein is an actin-associated protein involved in a range of processes dependent on cytoskeleton remodeling and cell polarity .

GFP marks VASP and VASP indicates actin in Focal formation.



Example 1. Vinculin Binding Stretching Activates Single Talin Rod Molecules

Science **323**, 638 (2009); Armando del Rio, *et al.*

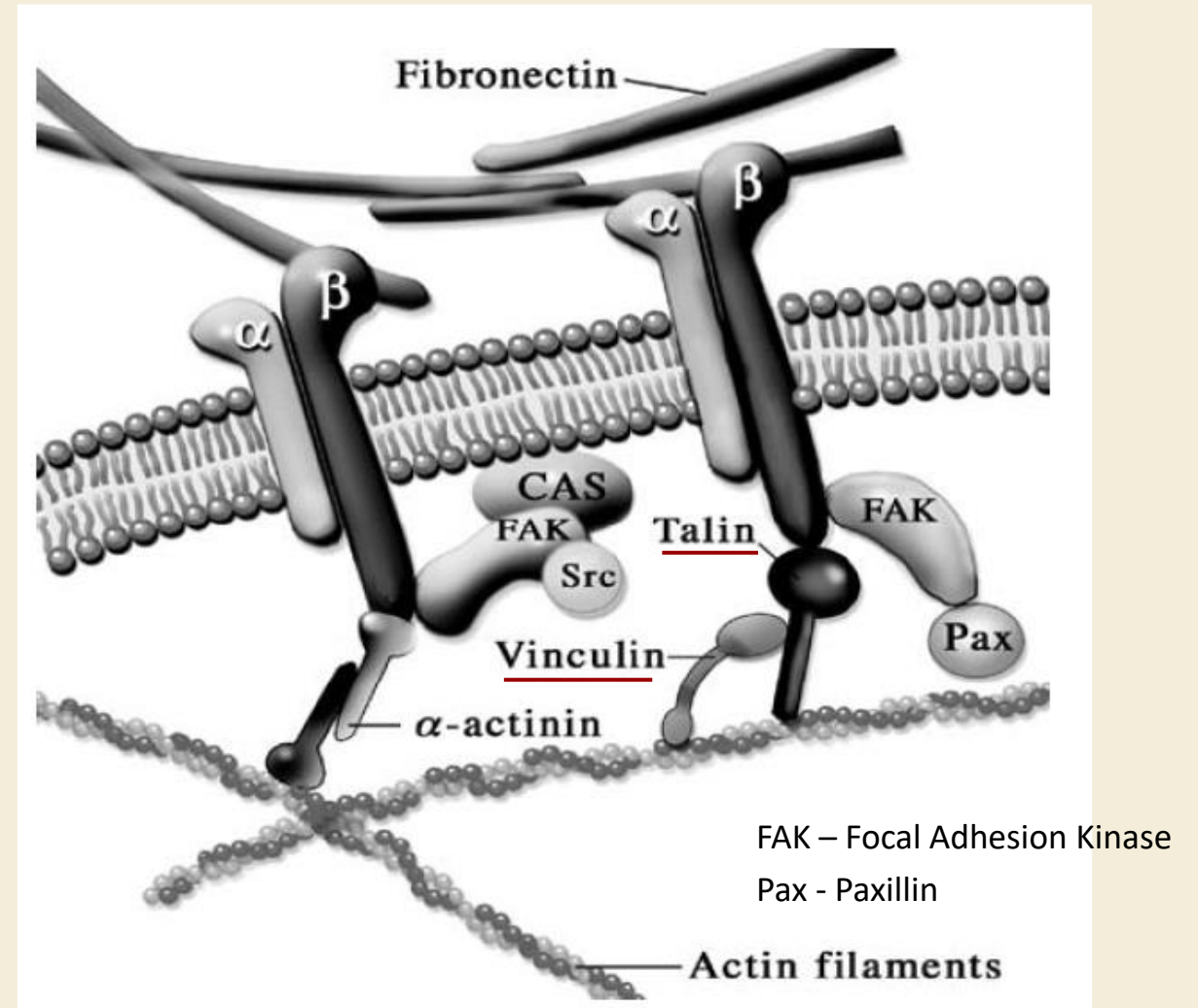
This work demonstrates how stretching of Talin can cause biochemical effect (Vinculin binding)

Known:

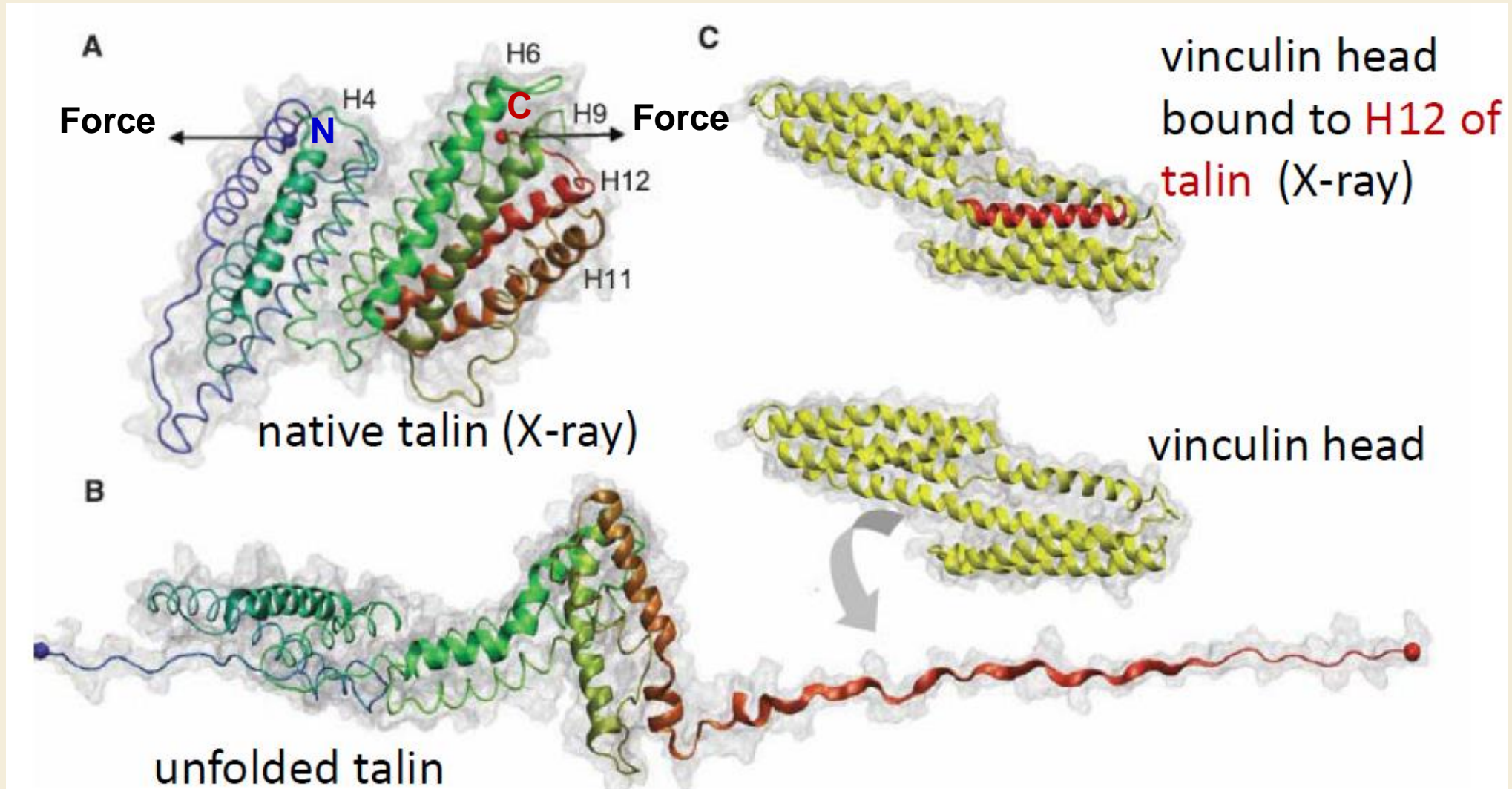
- Mechanical forces increase the accumulation of vinculin at the focal adhesions
- Talin can bind to the actin cytoskeleton

Hypotesis:

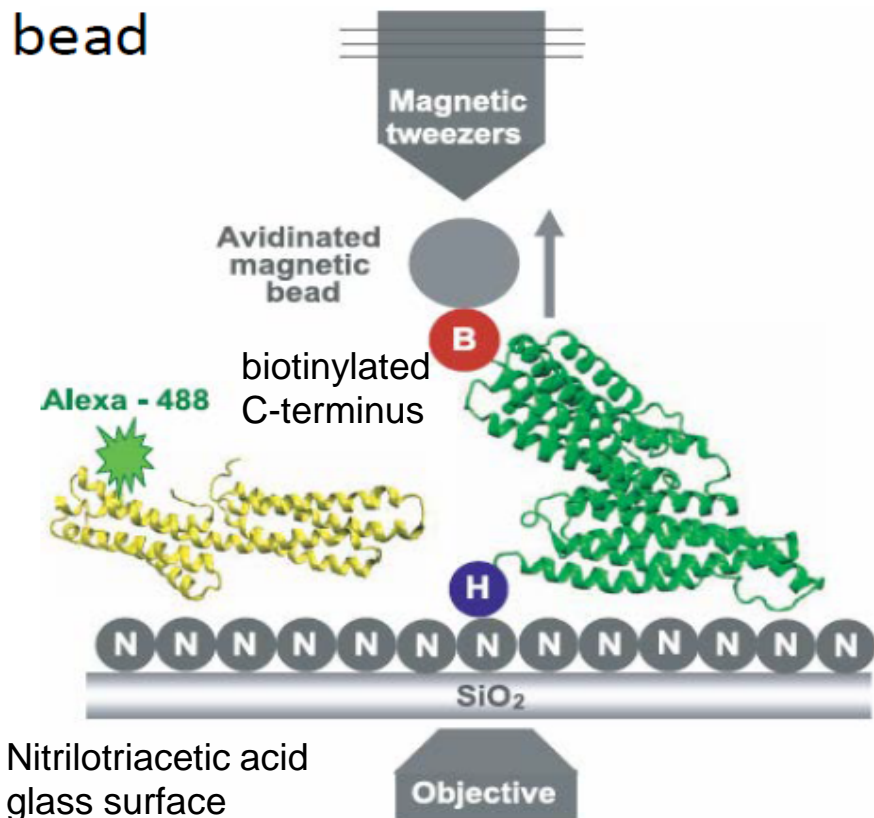
- a, b suggest that force induced by actomyosin contraction could stretch the talin rod exposing vinculin binding sites to the vinculin head.



Structure of the talin rod (TR) and proposed unfolding of the helical bundles in the TR and vinculin head binding to the helix H12 of TR - molecular dynamic simulations



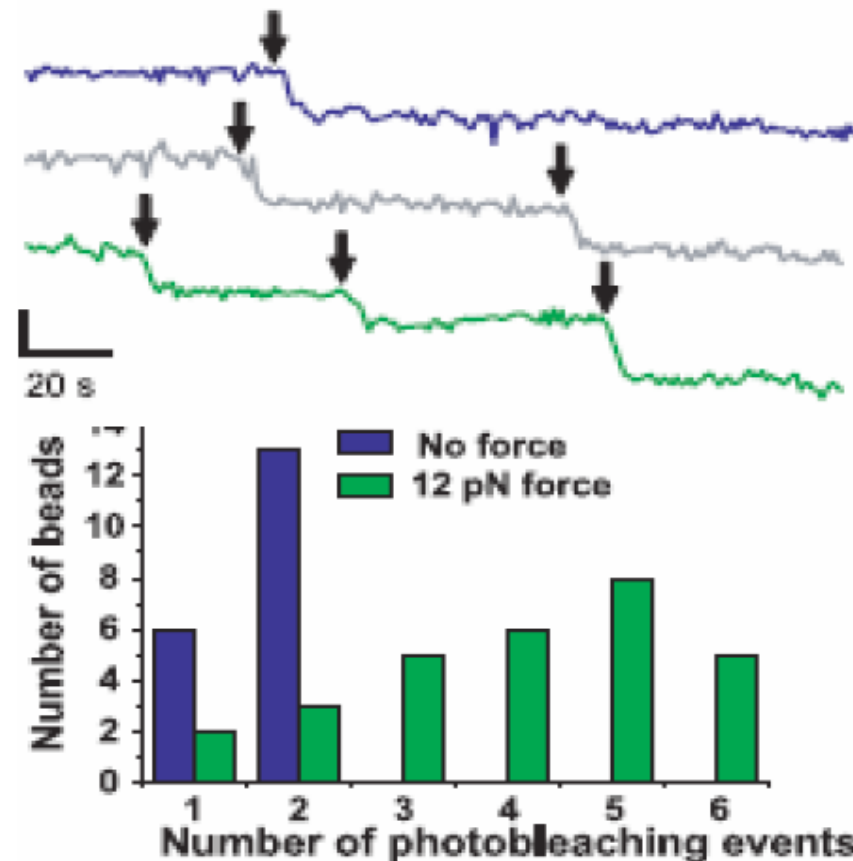
Pull on Talin with magnetic bead



Detect binding of fluorescent Vinculin

More Vinculin bind at Higher force

Detect number of bound vinculin by number of photobleaching events

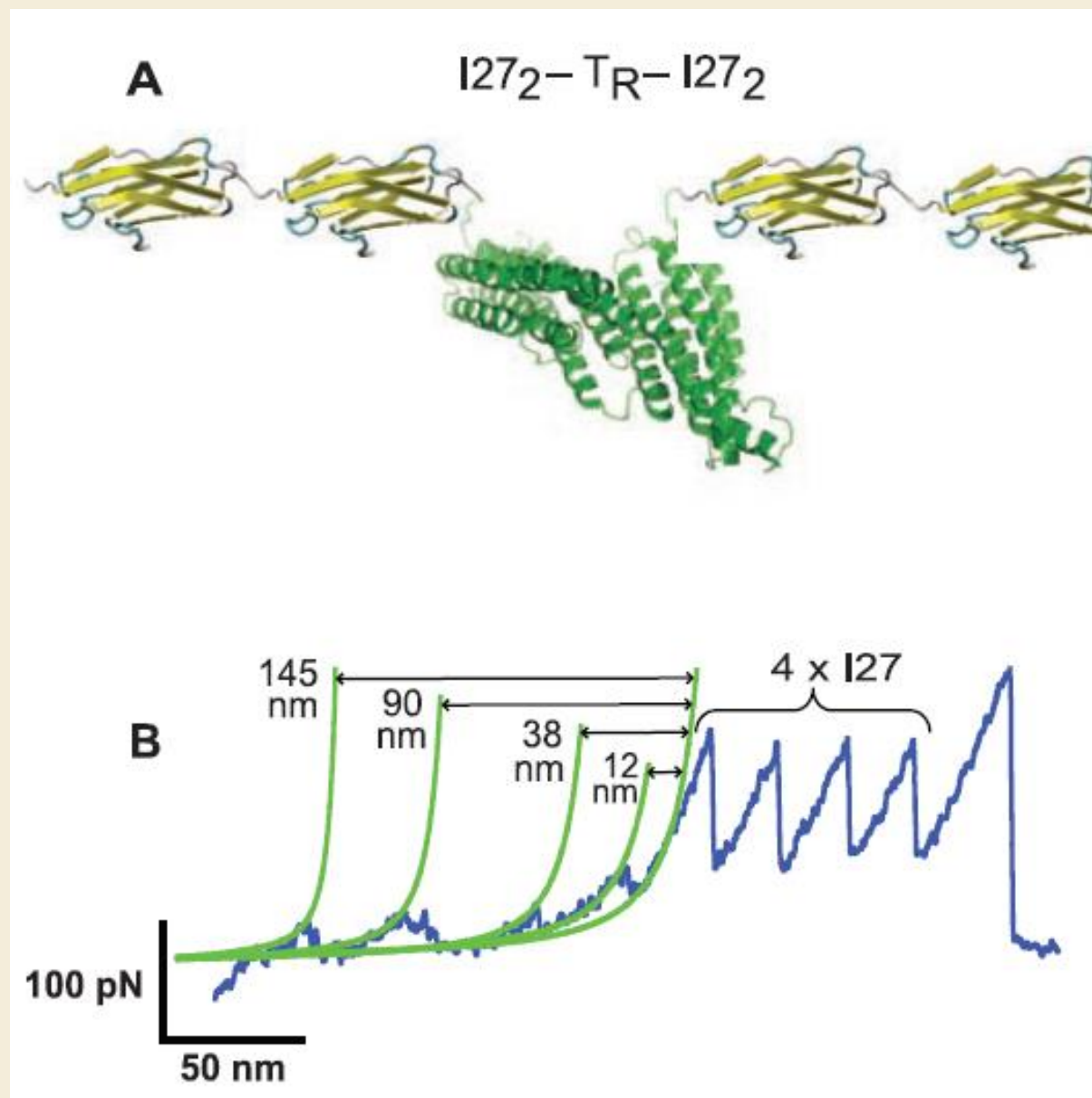


AFM force extension experiments.

(A) Diagram of the polyprotein designed for AFM

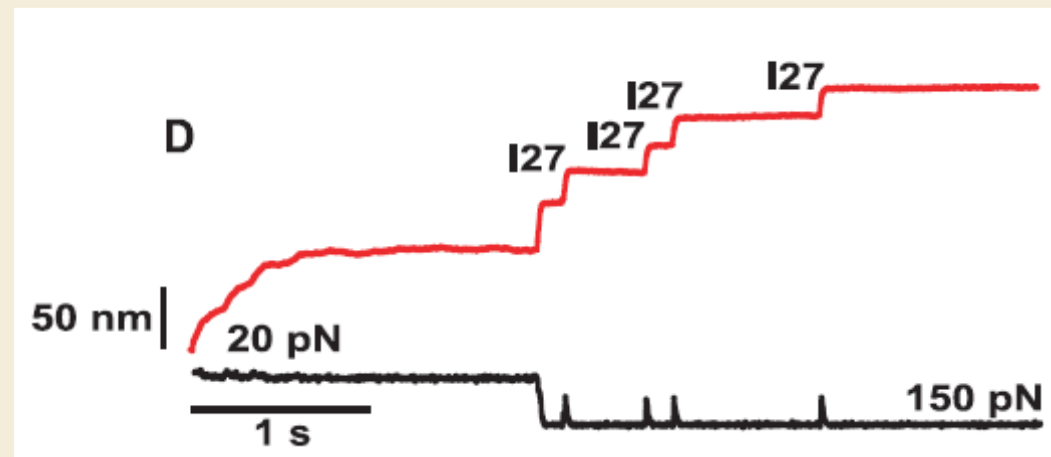
(B) Force extension trace for I272-TR-I272.

The force extension experiments provide a mechanical description for the TR unfolding forces and the contour lengths



AFM Force clamp spectroscopy to study the unfolding rate of TR:

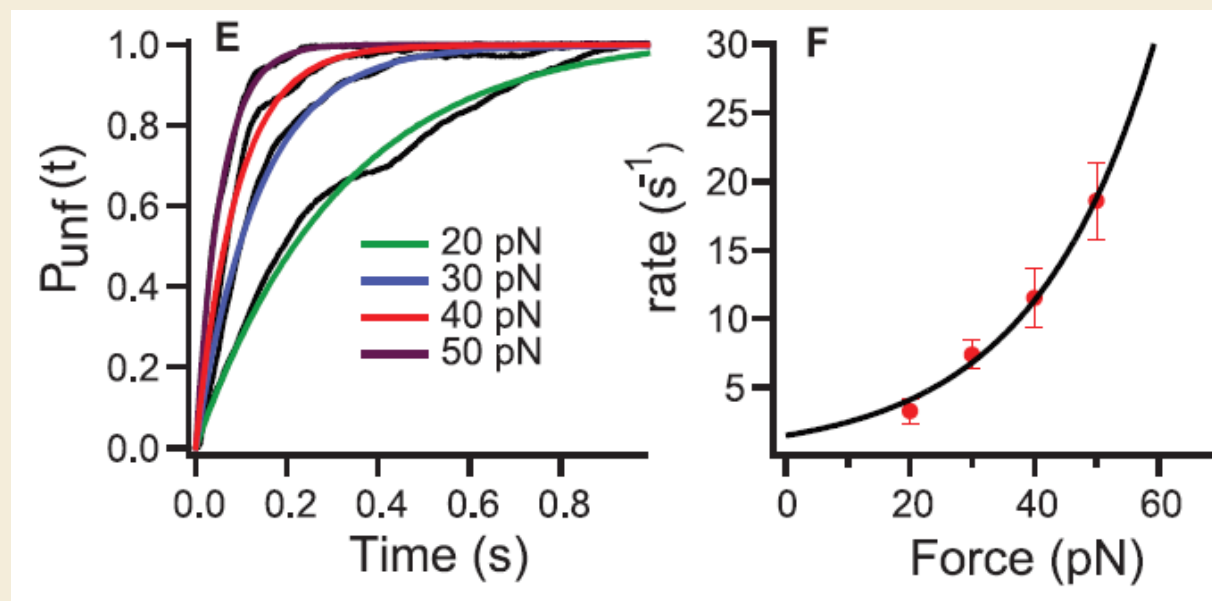
apply a constant calibrated force to a single TR for determining the unfolding trajectory as a function of time.



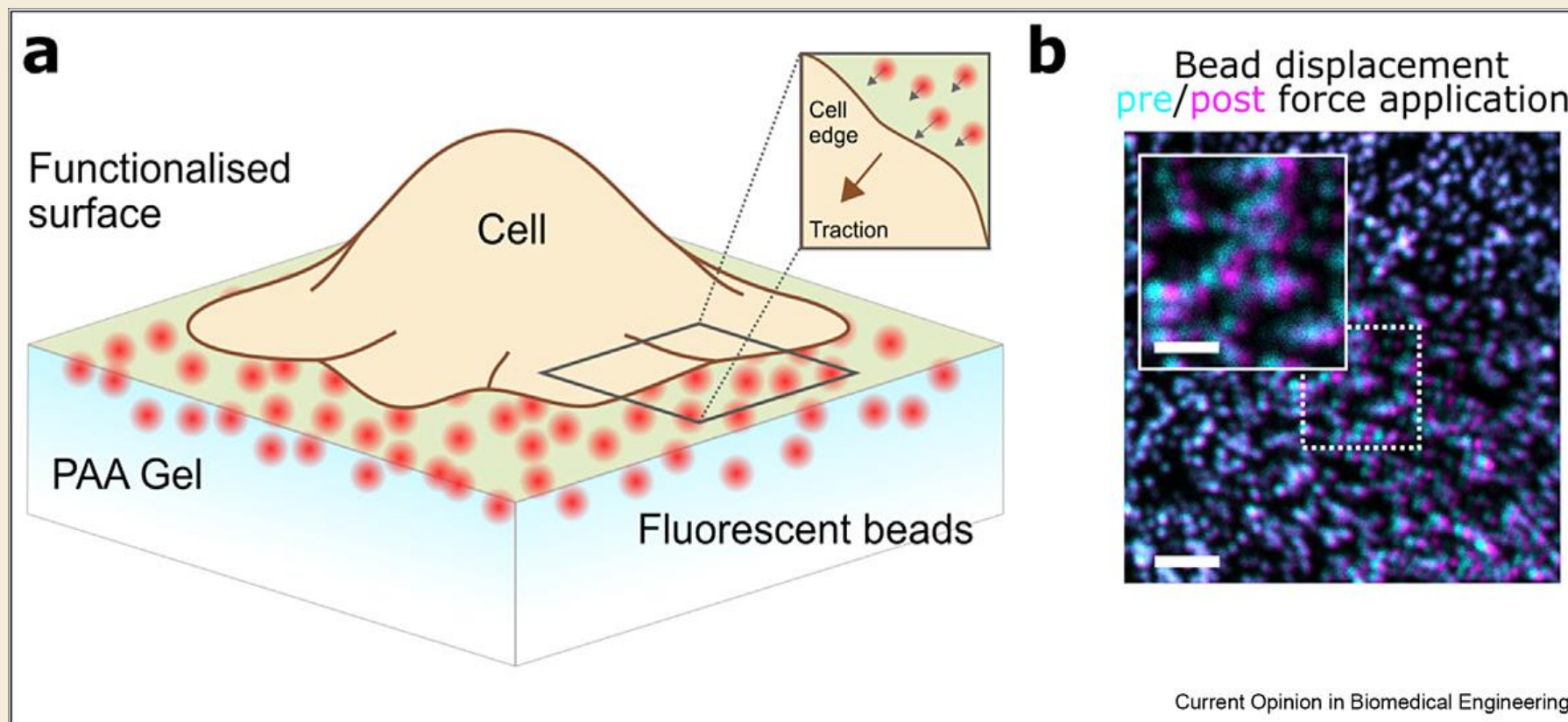
Probability of unfolding versus time for TR

And

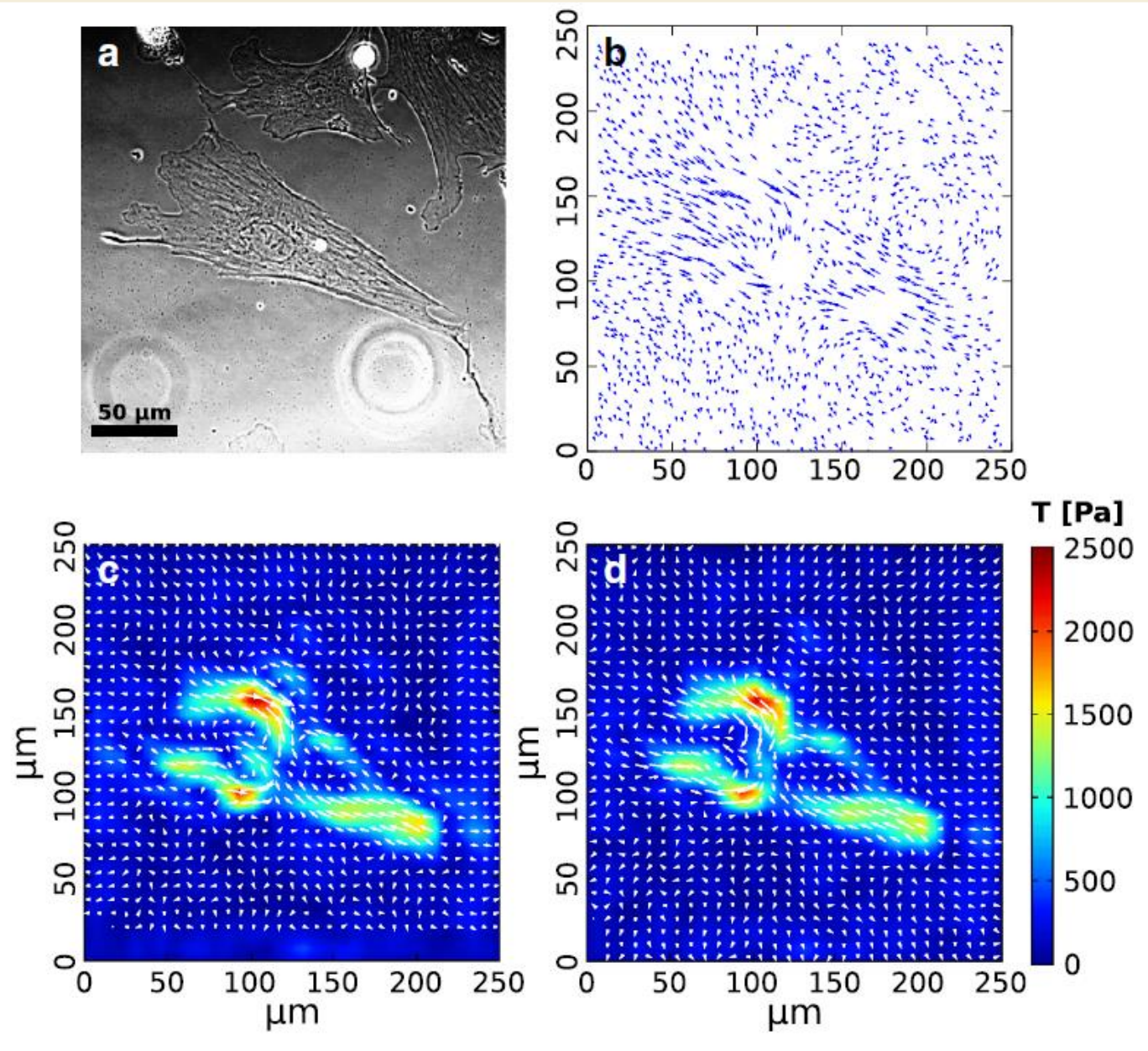
The rate constant of unfolding as a function of force



Example 2. Measuring the stress exerted by a cell on its substrate environment by Traction Force Microscopy (TFM)



Fluorescent nanobeads are embedded in a soft substrate (PAA - PolyAcrylAmide) with a known elastic modulus ($E=5-15$ kPa). Cells exert forces on the substrate, causing the beads displacement, which is tracked by image processing. The stress exerted on the substrate by the cells is reconstructed using the elastic body theory.

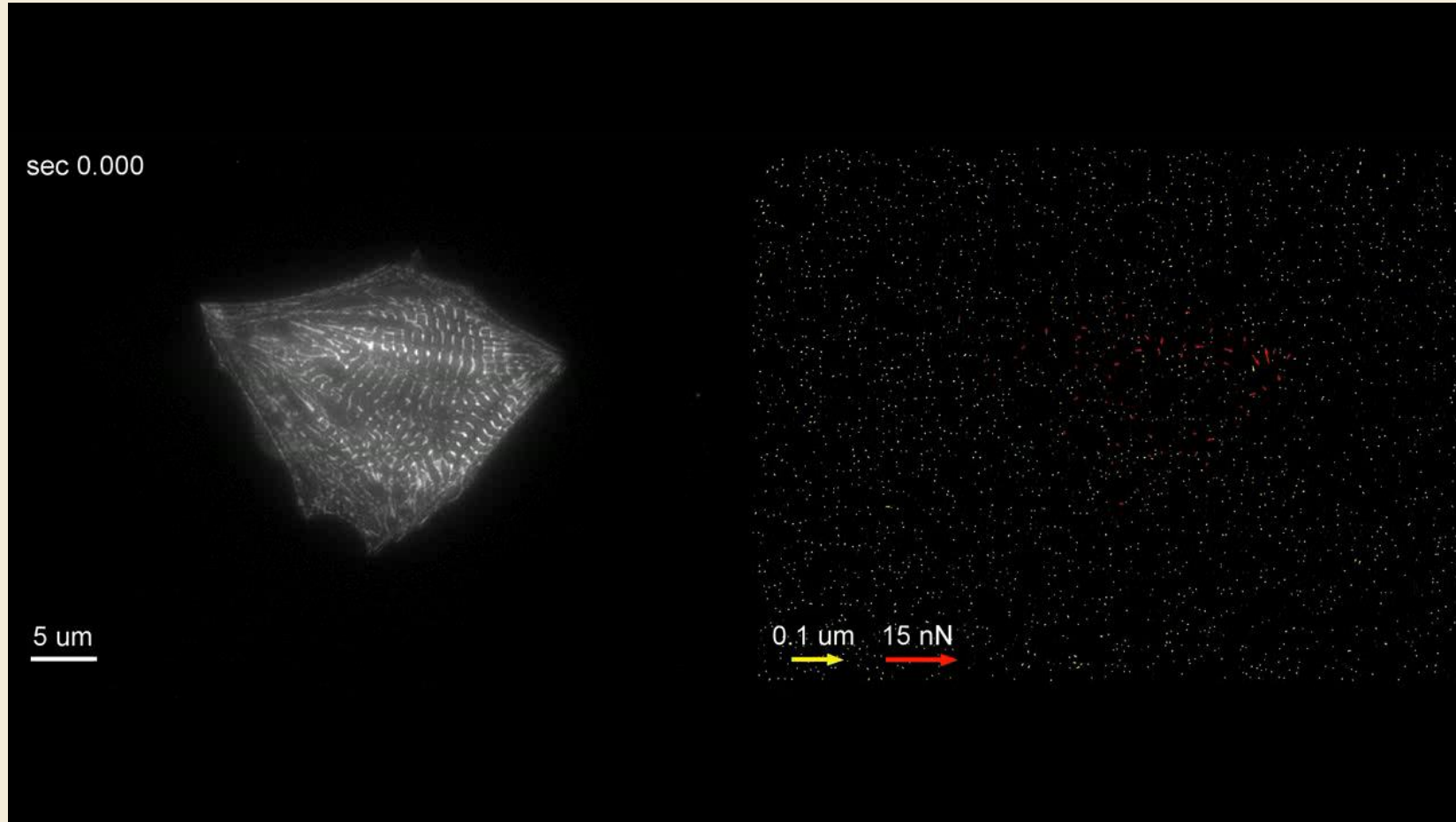


(a) Phase contrast image of a cardiac myofibroblast on an $E=15$ kPa PDMS-substrate. PDMS - Polydimethylsiloxane

(b) Substrate displacement field derived from the displacement of embedded fluorescent marker beads.

(c) Reg-FTTC (Regularized Fourier Transform Traction Cytometry) reconstruction.

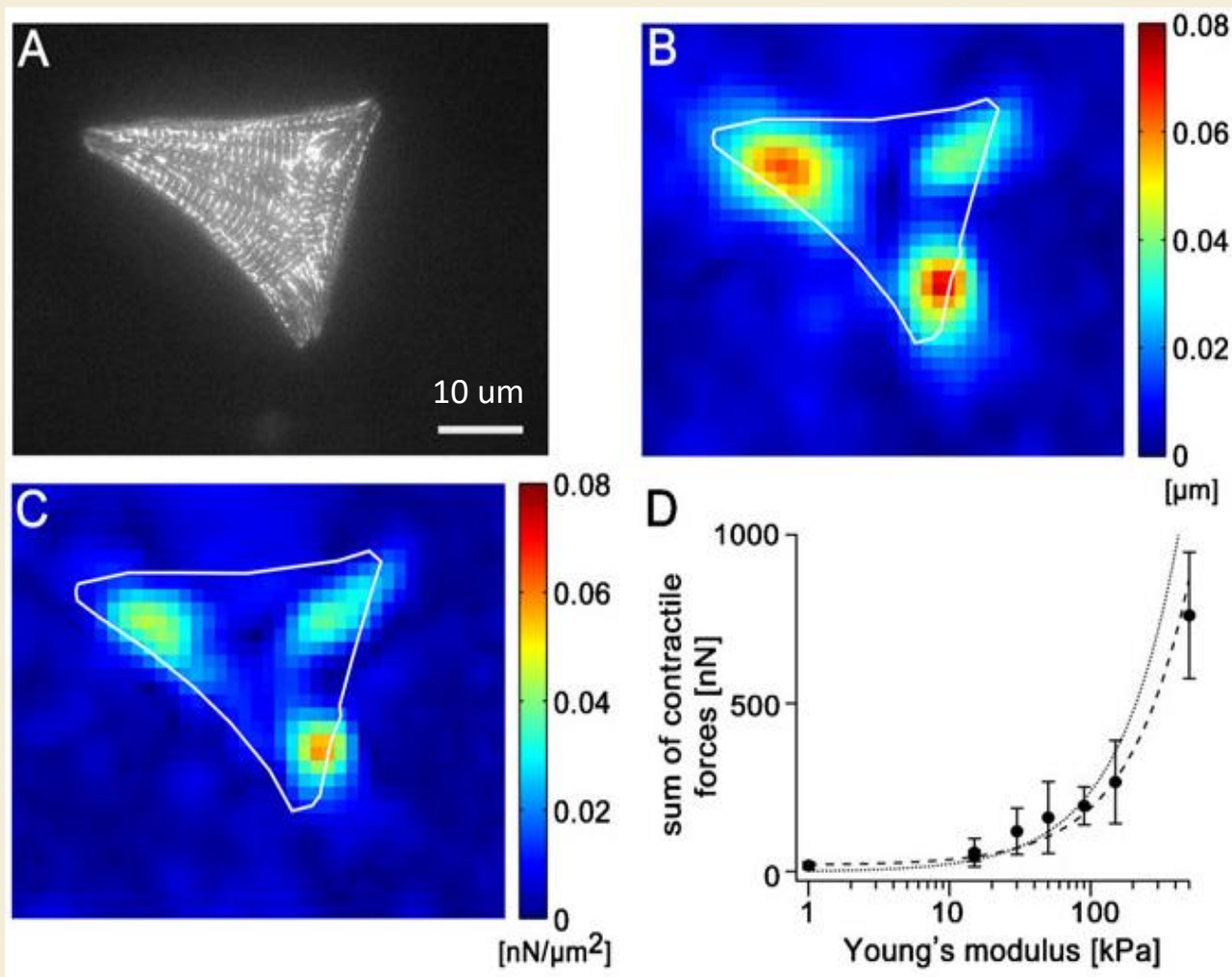
(d) FEM-based traction reconstruction.



Nils Hersch et al
Biology Open (2013), 2, 351,
doi: 10.1242/bio.20133830

Actinin transfected cardiomyocytes were grown on bead microstructured elastomeric substrate ($E = 30 \text{ kPa}$). Cells were analyzed in fluorescence for actinin localization (left) and bead displacement over time. Bead displacements were determined using image processing techniques (yellow arrows, right) and cell forces applied at interactively chosen FAs and costameres were calculated (red arrows, right).

Total force depends on substrate stiffness

**Force fields along the contractile apparatus.**

A) GFP-actinin transfected myocytes grown on bead micropatterned substrates with different Young's modulus

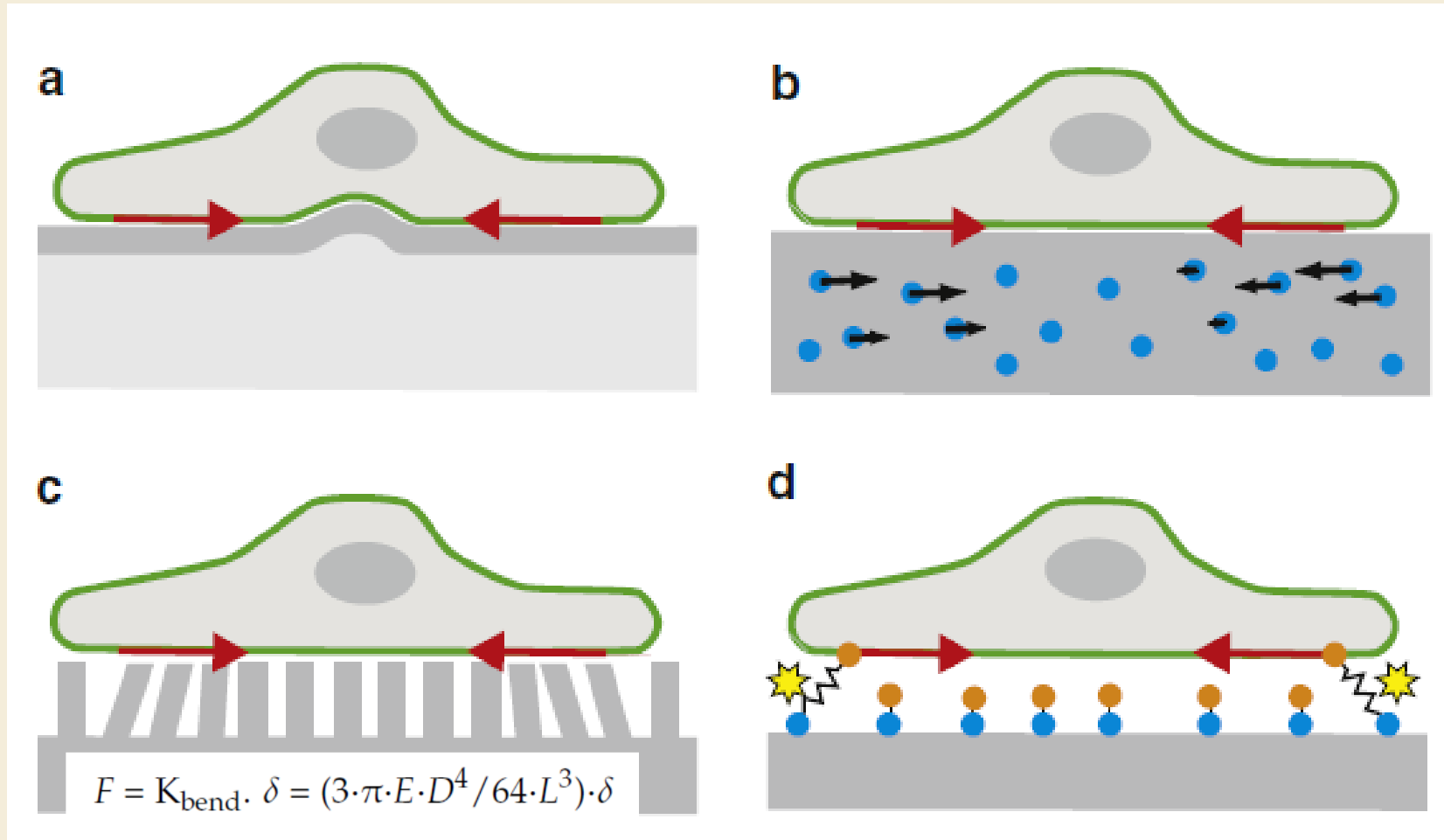
B) Measured substrate deformation fields

C) Reconstructed entire force fields

D) Total sum of contractile forces vs substrate elasticity: the sum of all maximum contractile forces were averaged over all cells analyzed per substrate elasticity ($n > 20$)

The dashed curve indicates a fitted linear force increase.

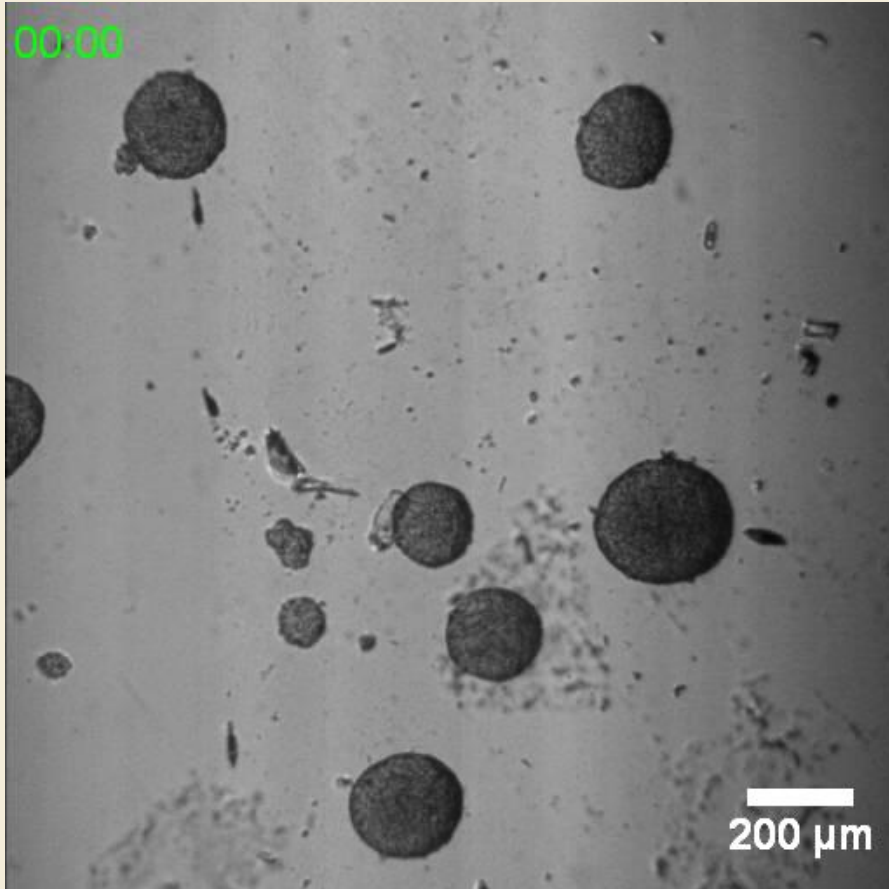
Different setups for traction force microscopy (TFM)



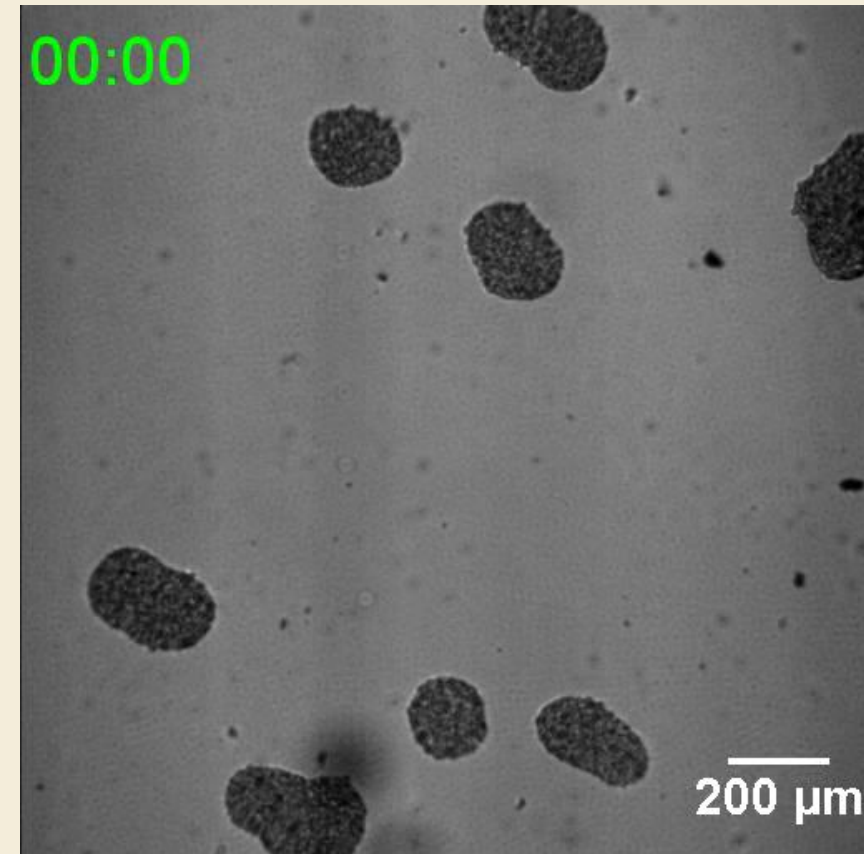
Schwarz & Soiné 2015 *Biochimica et Biophysica Acta - Molecular Cell Research*

- (a) Thin film buckles under cell traction (difficult to evaluate quantitatively);
- (b) Hydrogel substrate with embedded marker beads (most used, requires image processing and deconvolution);
- (c) Pillar arrays are local strain gauges and do not require deconvolution;
- (d) Fluorescent stress sensors typically use the relative movement of two molecular domains connected by a calibrated elastic linker to create a fluorescent signal, e.g. by Förster resonance energy transfer (FRET) or by quenching.

Cell motility / migration depends of the substrate properties: biochemical and mechanical



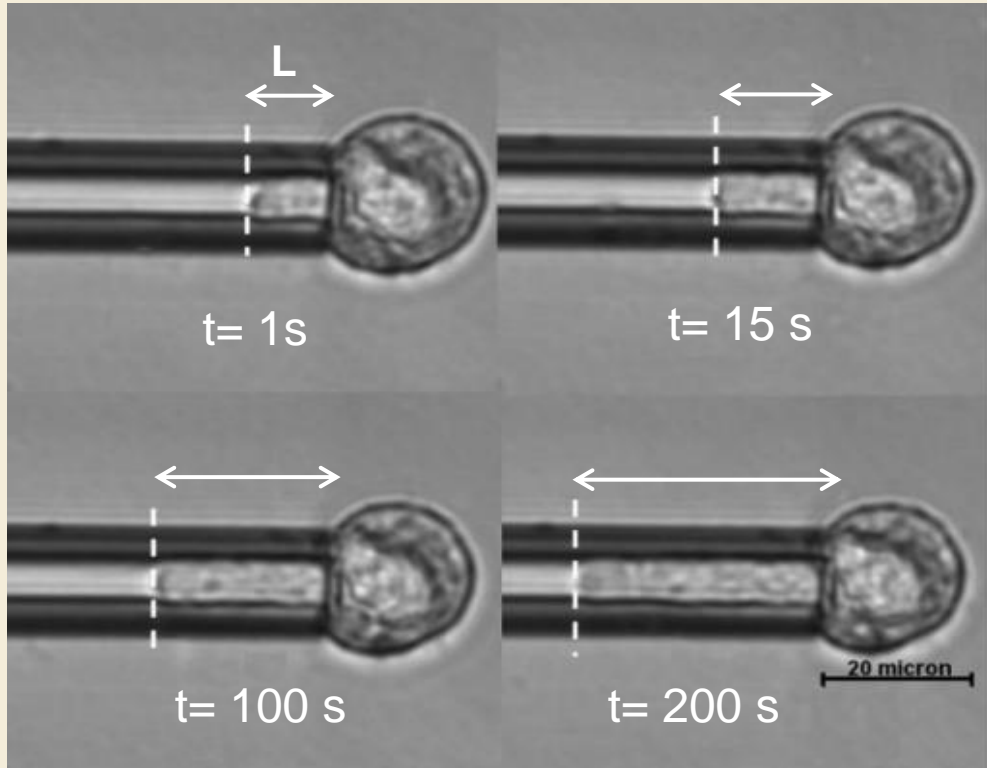
PAA gel – with biochemical gradient
 Substrate stiffness - 11 kPa
 Fibronectin at right , no fibronectin at left
 Cells migrate faster on fibronectin



PAA gel – with physical gradient
 Substrate stiffness:
 3 kPa right, 17 kPa left
 Cells migrate faster on harder substrate

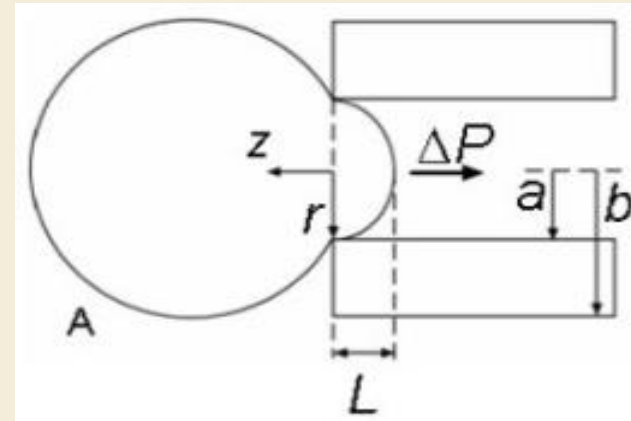
Example 3. Viscoelastic behaviour of human mesenchymal stem cells measured by Micropipette Aspiration

Micropipette aspiration of hMSCs

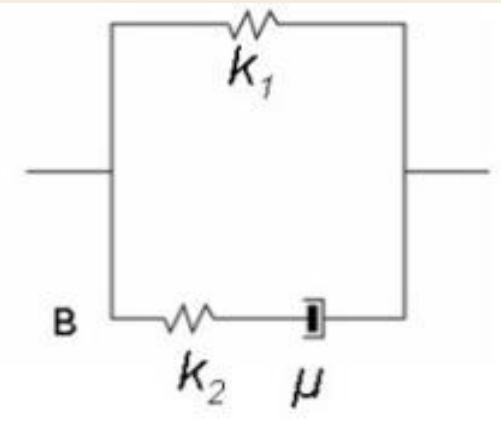


ΔP - suction pressure: 20 Pa – 300 Pa

Model of the micropipette aspiration test

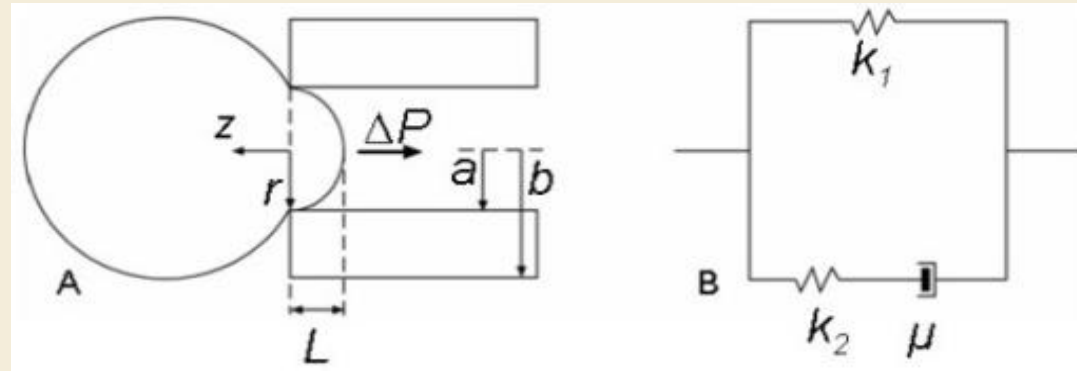


Viscoelastic model of the cell



k_1 – membrane local elasticity ,
 k_2 – membrane bending rigidity,
 μ - apparent viscosity.

Theoretical model of the micropipette aspiration test



Displacement $L(t)$ of the cell into the micropipette:

$$L(t) = \frac{\Phi a \Delta P}{\pi k_1} \left[1 - \frac{k_2}{k_1 + k_2} e^{-t/\tau} \right]$$

$$\mu = \frac{\tau k_1 k_2}{k_1 + k_2}$$

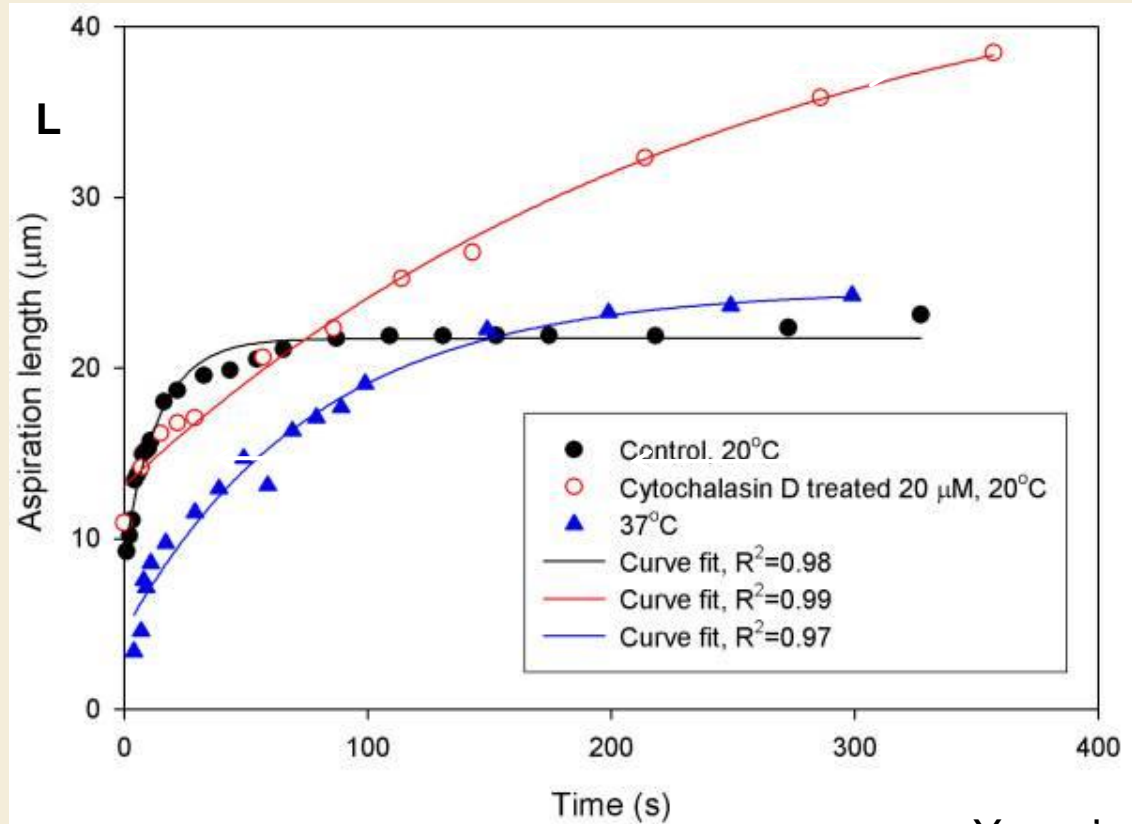
Apparent viscosity

$$E_0 = \frac{3}{2}(k_1 + k_2), \quad E_\infty = \frac{3}{2}k_1$$

E_0 - instantaneous Young's modulus,

E_∞ - equilibrium Young's modulus

Φ is a constant, the wall function, related to the ratio of the micropipette wall thickness to the pipette radius. $\Phi = 2$ here.



Experimental results for aspiration length L(t) vs time

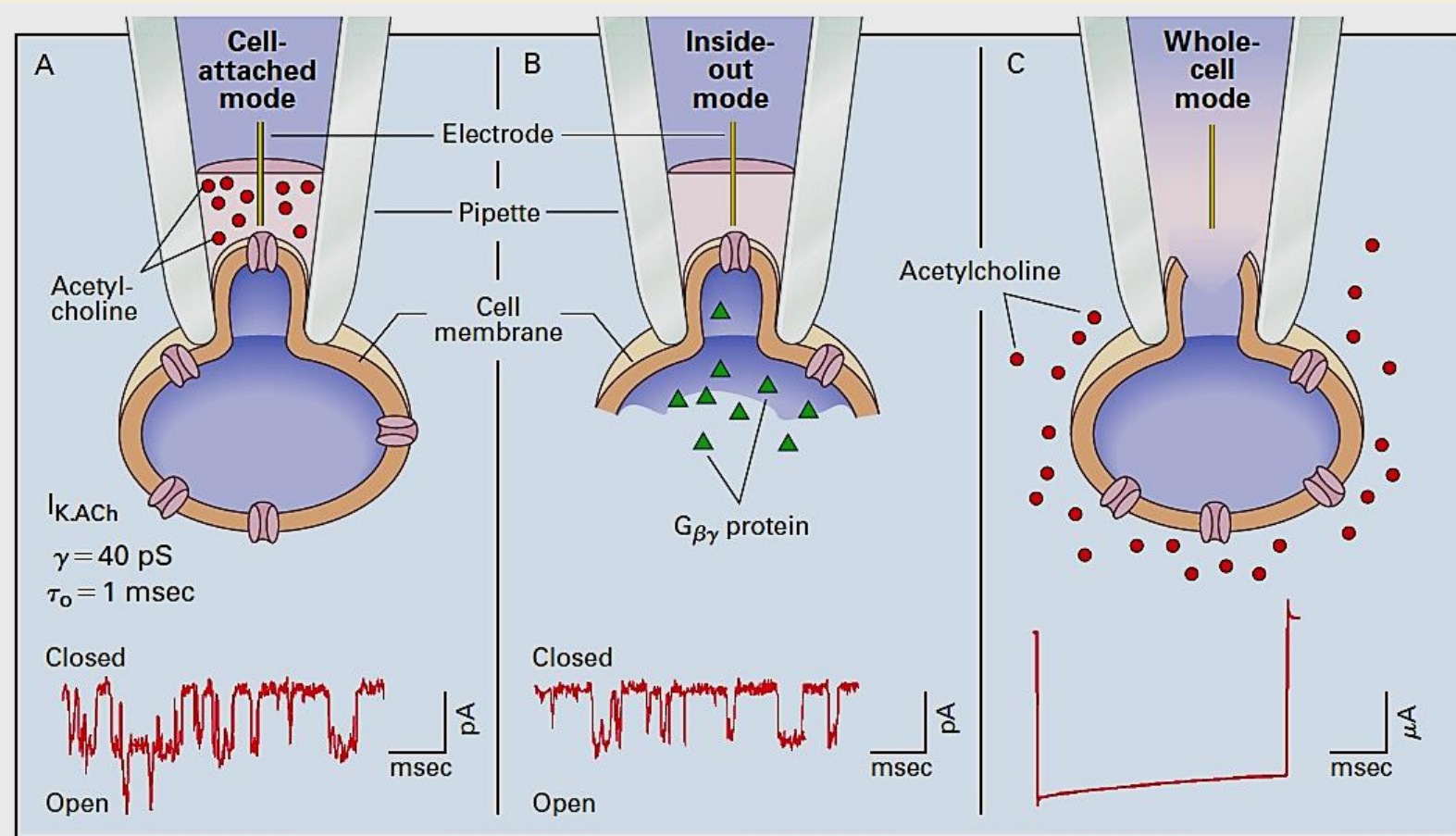
$$L(t) = \frac{\Phi a \Delta P}{\pi k_1} \left[1 - \frac{k_2}{k_1 + k_2} e^{-t/\tau} \right]$$

Young's modulus and viscosity for different cell types, measured by MA

Cell types	Mechanical properties		
	E_0 (Pa)	E_∞ (Pa)	μ (Pa·s)
Porcine endothelial	429	114 ± 35	8300 ± 4000
Human chondrocyte	640	270	2100
hMSC	886 ± 289	372 ± 125	2700 ± 1600

Pipette measurements are very much used in cell electrophysiology

Patch-Clamp Measurement of Ion-Channel Activity



1997-Ackerman and Clapham, Ion channels – basic science and clinical disease, New England J. of Medicine

Patch-Clamp Measurement of Ion-Channel Activity, with the Acetylcholine-Sensitive Potassium Channel ($I_{K.Ach}$) used as an example.

(A) **the “cell-attached” mode:** a pipette is pressed tightly against the cell membrane, suction is applied, and a tight seal is formed between the pipette and the membrane. The seal ensures that the pipette captures the current flowing through the channel.

In the cell-attached membrane patch, the intracellular contents remain undisturbed. Here, acetylcholine in the pipette activates the $I_{K.Ach}$, which has a characteristic open time (t_0) of 1 msec and a conductance (γ) of 40 picosiemens.

(B) **the inside-out mode:** after a cell-attached patch has been formed, the pipette is pulled away from the cell, ripping off a patch of membrane that forms an enclosed vesicle. The brief exposure to air disrupts only the free hemisphere of the membrane, leaving the formerly intracellular surface of the membrane exposed to the bath. Now the milieu of the intracellular surface of the channels can be altered. In this figure, adding purified $G_{\beta\gamma}$ protein to the exposed cytoplasmic surface activates the $I_{K.Ach}$.

(C) **the whole-cell mode,** after a cell-attached patch has been formed, a pulse of suction disrupts the membrane circumscribed by the pipette, making the entire intracellular space accessible to the pipette. Instead of disrupting the patch by suction, a pore-forming molecule, such as amphotericin B or nystatin, can be incorporated into the intact patch, allowing ions access to the interior of the cell but maintaining a barrier to larger molecules. In this figure, the net current ($I_{K.Ach}$) after the application of acetylcholine is shown.



2020 KAVLI PRIZE IN NEUROSCIENCE

*“for their transformative discovery of
receptors for temperature and pressure.”*

Ardem Patapoutian

Scripps Research,
La Jolla, US

David Julius

University of California,
San Francisco, US

While neural mechanisms for sensing chemicals in olfaction, light in vision, acoustic waves in hearing have been described, a molecular basis for how temperature and pressure are detected and encoded into electrical signals has been lacking.

The two Kavli Prize Laureates, Julius and Patapoutian, discovered receptors for temperature and pressure, two critical physical features of the environment.

These findings revolutionized the field of neuroscience by providing a molecular and neural basis for thermosensation and mechanosensation.

In 2010, Patapoutian and his team discovered two new ion channels that were activated by mechanical pressure (a gentle poke with a fine rod), to produce electrical activity. They cloned and named the ion channels PIEZO1 and PIEZO2.

PIEZO1 and PIEZO2 were found on sensory neurons and other cell types, leading to an explosion of research on the role of these ion channels in pressure sensation for touch, pain, blood pressure regulation, lung inflation, and proprioception.

Proprioception refers to our ability to sense where our body is in space. It normally enables us to stand and walk, even with our eyes closed or blindfolded, and depends on neurons that signal muscle stretch to the brain. Patapoutian's team and others have shown that PIEZO2 is the key receptor involved, with reports that humans with a rare deficiency in PIEZO2 have difficulty standing and walking in the dark. They also do not experience pain hypersensitivity.

Patapoutian's more recent research in human genetics and mouse models has demonstrated a role for PIEZO1 in controlling red blood cell volume. He found a PIEZO1 gene variant that appears to protect against infection by the malaria parasite, and is carried by one in three people of African descent.

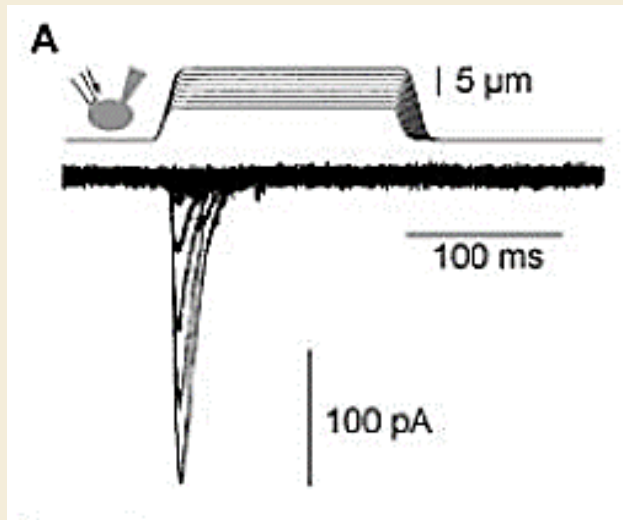
Science. 2010 October 1; 330(6000): 55–60. doi:10.1126/science.1193270.

Piezo1 and Piezo2 are essential components of distinct mechanically-activated cation channels

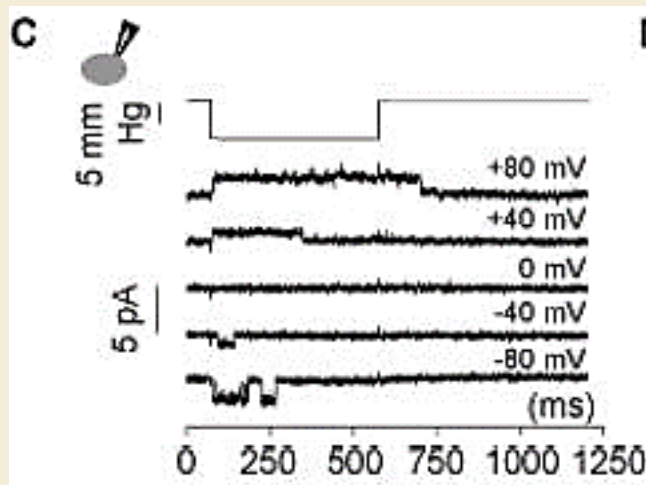
Bertrand Coste¹, Jayanti Mathur², Manuela Schmidt¹, Taryn J. Earley¹, Sanjeev Ranade¹, Matt J. Petrus², Adrienne E. Dubin¹, and Ardem Patapoutian^{1,2,3}

¹Department of Cell Biology, The Scripps Research Institute, La Jolla, CA 92037

²Genomics Institute of the Novartis Research Foundation, San Diego, CA 92121



(A) Representative traces of mechanically-activated (MA) inward currents expressed in Neuro2A (N2A) cells. Cells were subjected to a series of mechanical steps of 1 μm movements of a stimulation pipette (inset drawing, arrow) in the whole-cell patch configuration at a holding potential of -80 mV .



(C) Single-channel currents (cell attached patch configuration) induced by negative pressure with a pipette (inset drawing, arrow) at holding potentials ranging from -80 mV to $+80\text{ mV}$ in a N2A cell.

Mechanical activation and the structure of these channels are still to be deciphered.

Force-induced conformational changes in Piezo1

Yi-Chih Lin^{1,#}, Yusong R Guo^{2,#}, Atsushi Miyagi¹, Jesper Levring², Roderick MacKinnon^{2,*},
Simon Scheuring^{1,*}

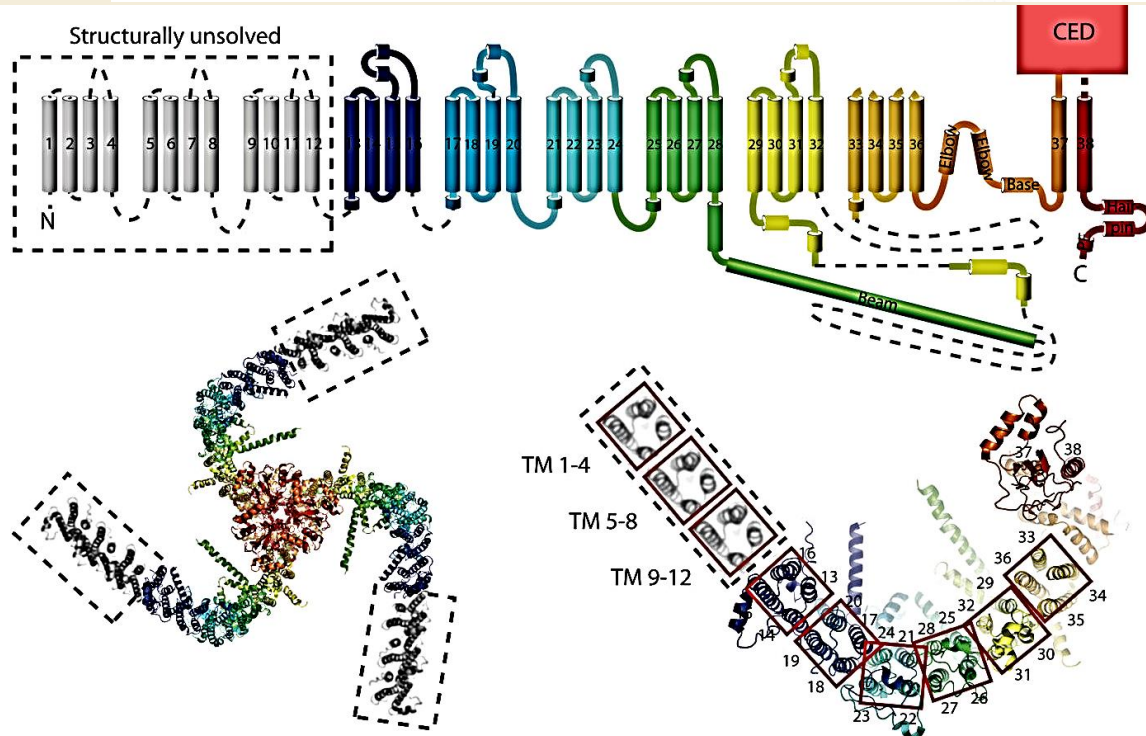
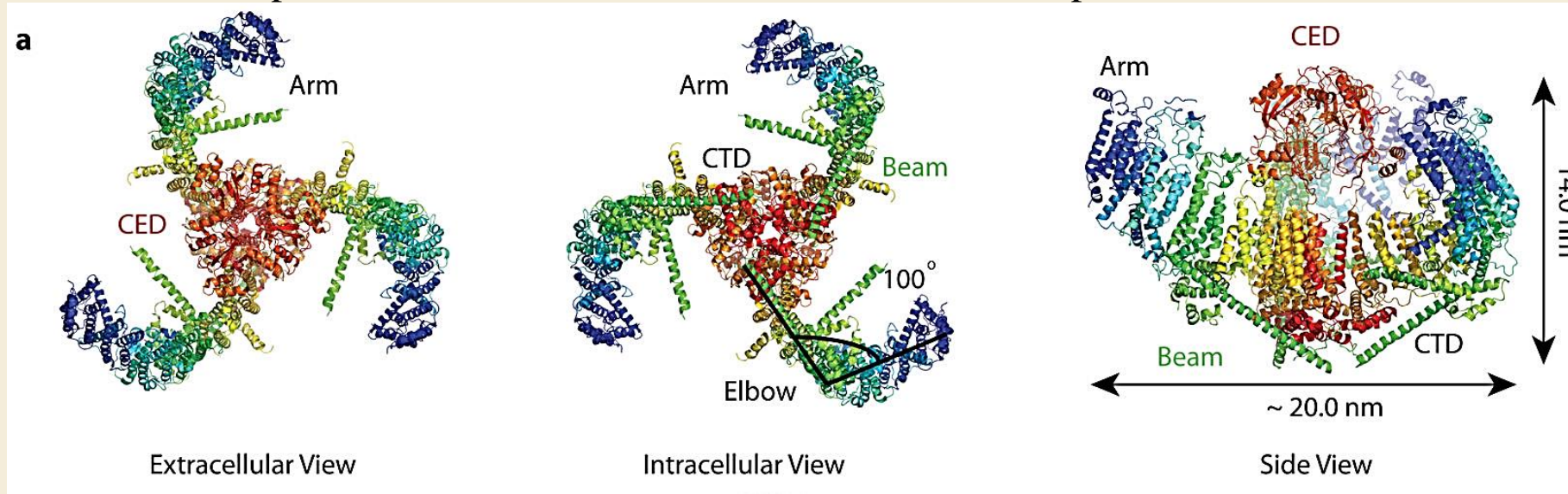
¹Department of Anesthesiology, Department of Physiology and Biophysics, Weill Cornell
Medicine, New York, United States

²Laboratory of Molecular Neurobiology and Biophysics, Howard Hughes Medical Institute, The
Rockefeller University, New York, United States

Nature. 2019 September ; 573(7773): 230–234. doi:10.1038/s41586-019-1499-2.

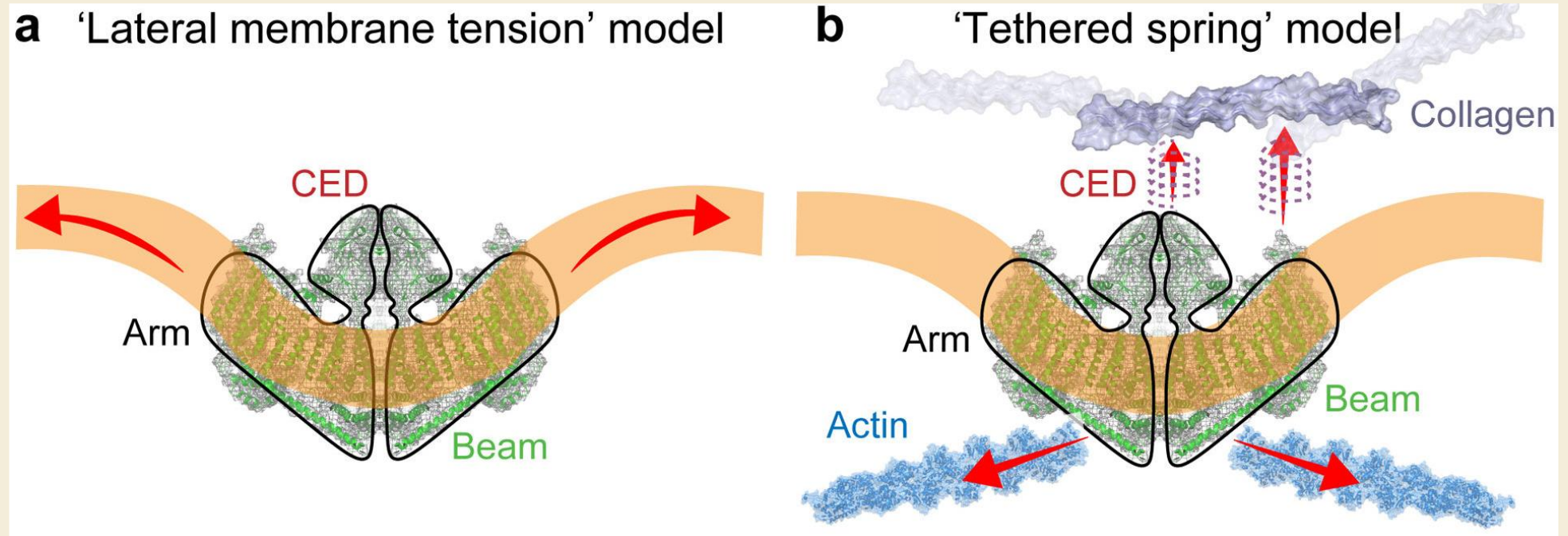
Partial molecular structures show a bowl-shaped trimer with extended arms. Here we use cryo-electron microscopy (cryo-EM) to show that Piezo1 adopts different degrees of curvature in lipid vesicles of different size. We also use high-speed atomic force microscopy (HS-AFM) imaging to analyze the deformability of Piezo1 under force in membranes on a mica surface: Piezo1 can be flattened reversibly into the membrane plane. By approximating the absolute force applied, we estimate a range of values for a mechanical spring constant for Piezo1. Both methods demonstrate that Piezo1 can deform its shape towards a planar structure. This deformation could explain how lateral membrane tension can be converted into a conformation-dependent free energy change to gate the Piezo1 channel in response to mechanical perturbations.

Top, bottom and side views of Piezo1 in cartoon representation



Topology of Piezo1, rainbow-colored with N-terminus in blue and C-terminus in red, except for structurally unsolved TM 1–12 regions in grey. Helices are represented as cylinders, loops as solid lines, and unresolved regions as dotted lines.

Top view of TMs, labeled as in the topology. Red squares outline 4-TM units that constitute the arm. TM 21–24 is at the ‘elbow’ of the arm. The hypothetical position of the unresolved units TM 1–4, TM 5–8 and TM 9–12 are indicated (dashed outline).



CED : C-terminal extracellular domain

Proposed activation mechanisms of Piezo1.

- (a) Lateral membrane tension model: Changes in membrane properties, e.g. tension or curvature, lead to a gating force applied onto Piezo1.
- (b) Tethered spring model: Piezo1 channel is activated through interactions with the cytoskeleton or the extracellular matrix. Red arrows indicate force application.

Results:

- the stiffness constant K of the protein would be ~ 32.5 pN/nm (~ 7.9 KT/nm²),
- the work to bring about the conformational change from curved to flat would be ~ 625 pN nm (~ 150 KT),
- the tension associated with half activation would be $\gamma \cong 1.9$ KT/nm²
- Piezo1 can undergo a reversible, flattening deformation when force is applied.

Try to understand and explain:

The experimental approach of HS-AFM, i.e. How forces are applied, how deformation is measured how energies are calculated and the the deformation model elaborated.

ARTICLE

Received 22 Feb 2016 | Accepted 16 Aug 2016 | Published 3 Oct 2016

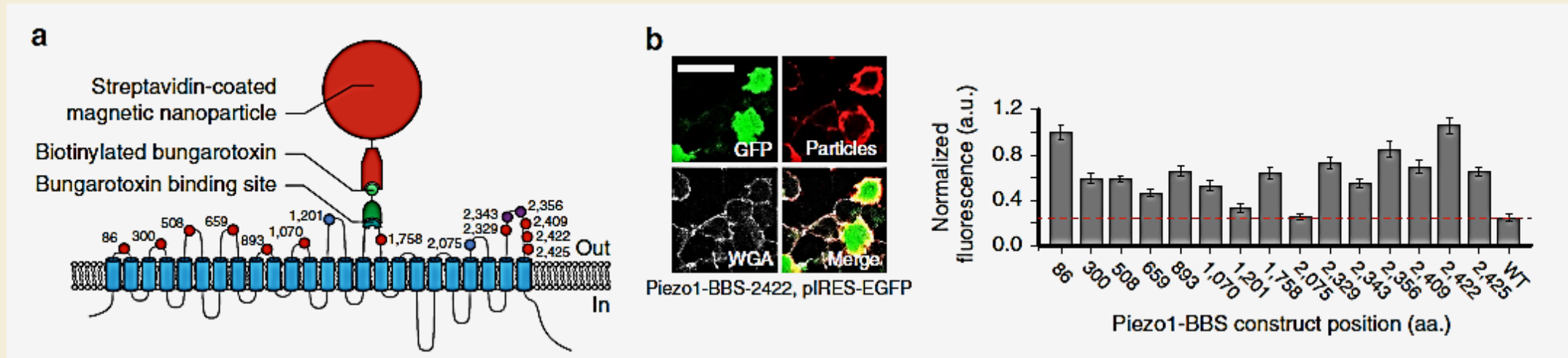
DOI: [10.1038/ncomms12939](https://doi.org/10.1038/ncomms12939)

OPEN

Localized force application reveals mechanically sensitive domains of Piezo1

Jason Wu¹, Raman Goyal¹ & Jörg Grandl¹

... we use magnetic nanoparticles as localized transducers of mechanical force in combination with pressure-clamp electrophysiology to identify mechanically sensitive domains important for activation and inactivation.



Localized force application by nanoparticle labelling and magnetic field generation.

IT allows to bind and apply forces at different domains of the protein !

- (a) Piezo1 transmembrane topology with aa. locations of BBS insertions (red, labelled and functional; blue, non-labelled; magenta, non-functional) and schematic of bead labelling strategy.
- (b) Representative images of HEK293T cells expressing Piezo1-BBS-2422-pIRES-EGFP construct, live-labelled with streptavidin-coated nanoparticles, immunostained against streptavidin, and labelled with WGA to confirm membrane localization (green, GFP; red, anti-streptavidin; grey, WGA). Mean fluorescence intensity normalized to BBS-86 (a.u.) of nanoparticle labelling along the cell membrane for all constructs compared with wild-type Piezo1 (WT, red line) ($n=10$ cells per transfection, 2–5 transfections; $P < 0.0001$ for all constructs except BBS-1201 and BBS-2075 ($P < 0.01$), one-way ANOVA and NP multiple comparison).

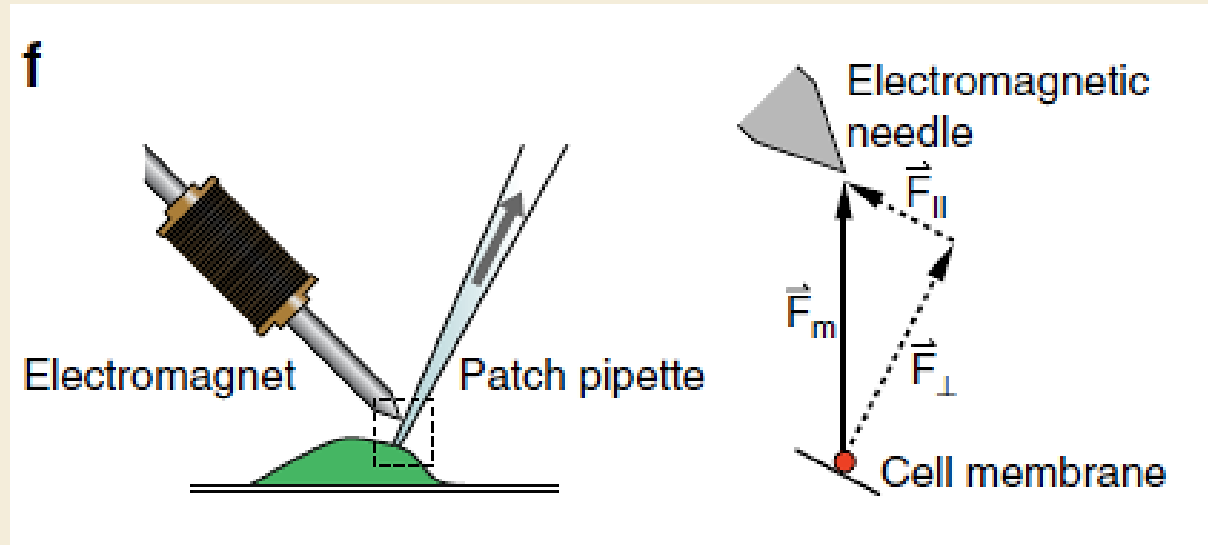
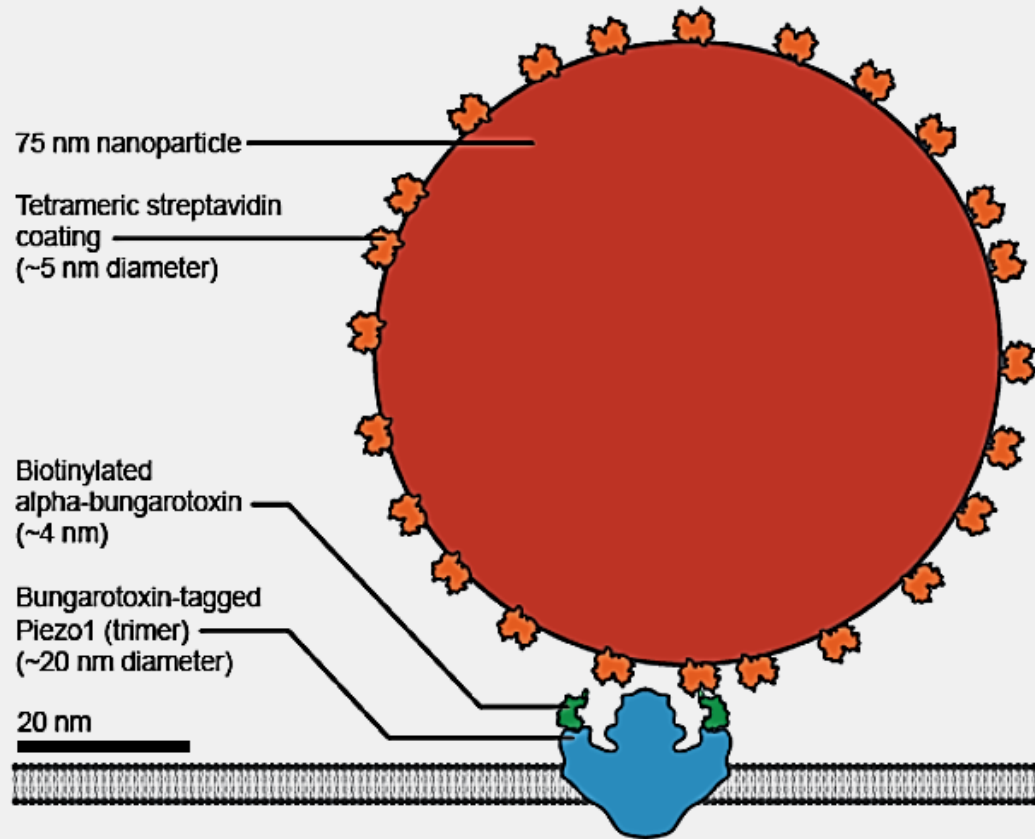


Diagram of patch-clamp pipette and electromagnetic needle

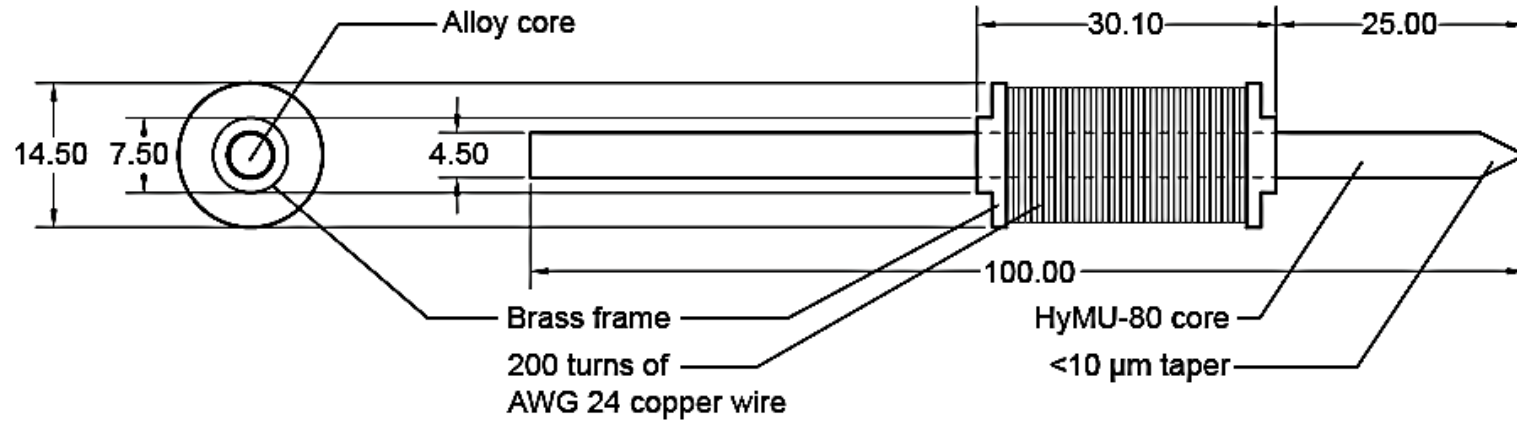
and corresponding force diagram on nanoparticle (F_m , magnetic force vector; F_\perp , force vector normal to patch membrane; F_\parallel , force vector parallel to patch membrane).



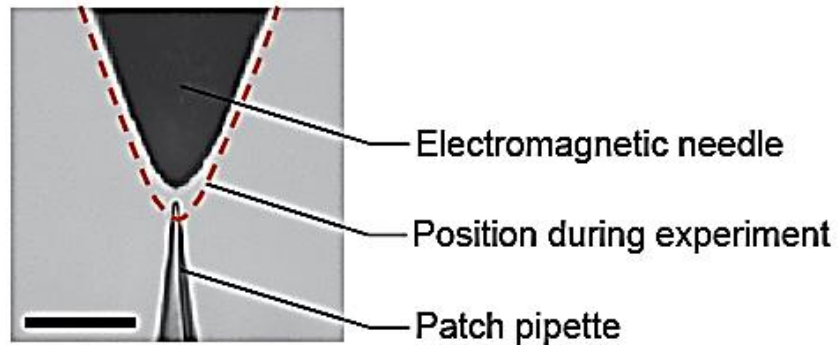
Scale diagram of BBS-Piezo1 binding complex.

Diagram depicting to-scale relationships of BBS-Piezo1, biotinylated bungarotoxin, and streptavidin-coated nanoparticle in complex.

a



b



Design of electromagnetic needle.

- (a) Design specifications for electromagnetic needle (units in mm).
- (b) Image of electromagnetic needle tip and patch pipette tip at 40x magnification. Dotted red line denotes position of needle above pipette tip during recording experiments. Scale bar is 50 μm .

Try to understand and explain:

The experimental approach to apply forces with EM needle, fluorescence imaging and patch clamp to measure ionic currents.

CELL MECHANICS

1. Introduction - L1

2. Physical principles

- 2.1. Forces at molecular and cell level - L2
- 2.2. Thermal forces, diffusion, and chemical forces;
and Single molecule experiments – L3, L4, L5, L6

3. Mechanics of the Cytoskeleton and Mechano-transduction

- 3.1. Motor proteins - types, working principle – L8-9
- 3.2. Force generation by the cytoskeleton and cell motility – L10

4. Experimental techniques to study cell mechanics

4.1. Cellular mechanotransduction (basic principles and examples) L11

- 4.2. Optical, magnetic and acoustic tweezers L7, L12
- 4.3. Super resolution optical microscopy techniques (STED, PALM) L12

- Lab visit and experimental optical tweezers cell mechanics session at CNR IOM

CELL MECHANICS

1. Introduction - L1

2. Physical principles

- 2.1. Forces at molecular and cell level - L2
- 2.2. Thermal forces, diffusion, and chemical forces;
and Single molecule experiments – L3, L4, L5, L6

3. Mechanics of the Cytoskeleton and Mechano-transduction

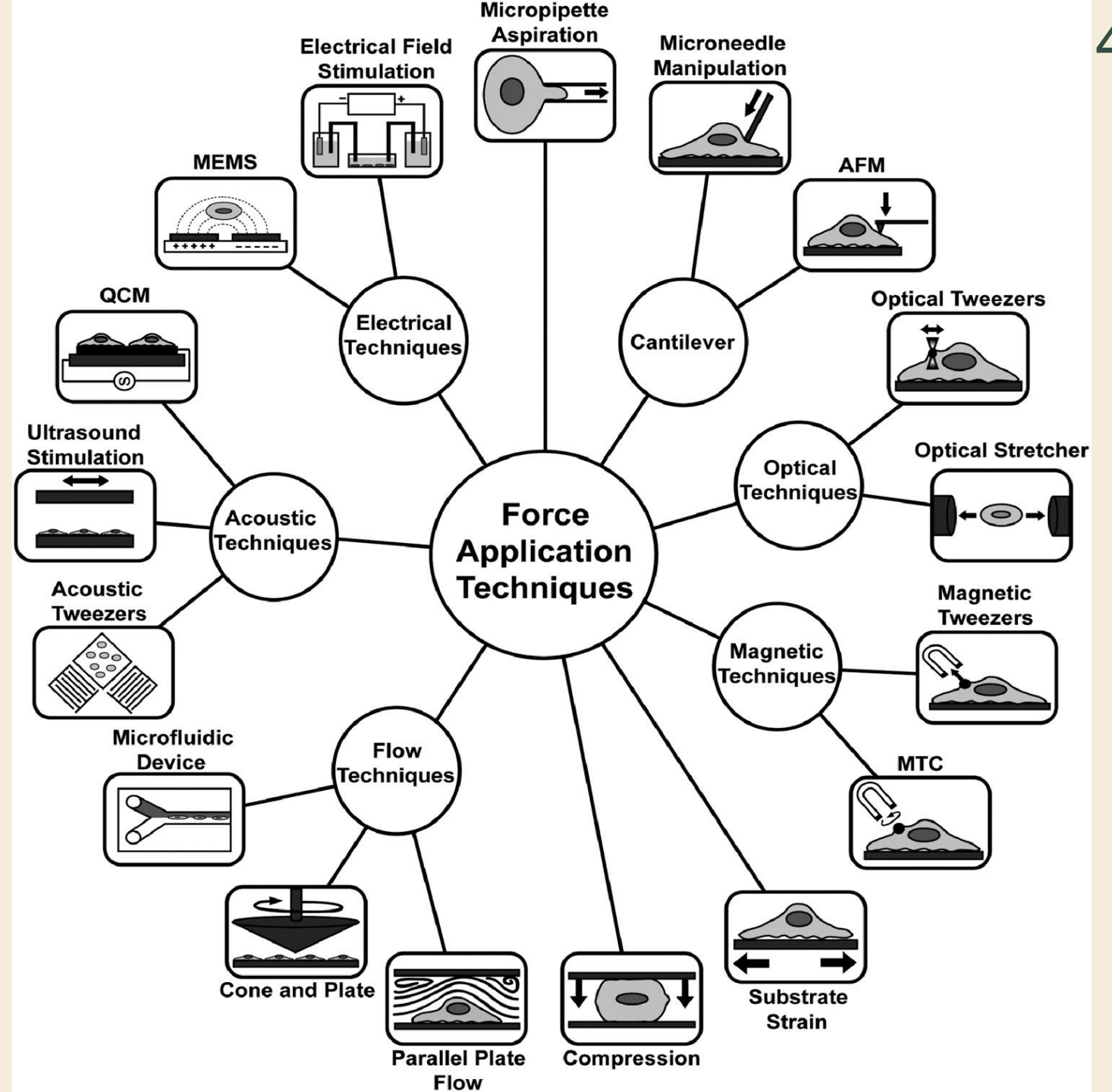
- 3.1. Motor proteins - types, working principle – L8-9
- 3.2. Force generation by the cytoskeleton and cell motility – L10

4. Experimental techniques to study cell mechanics

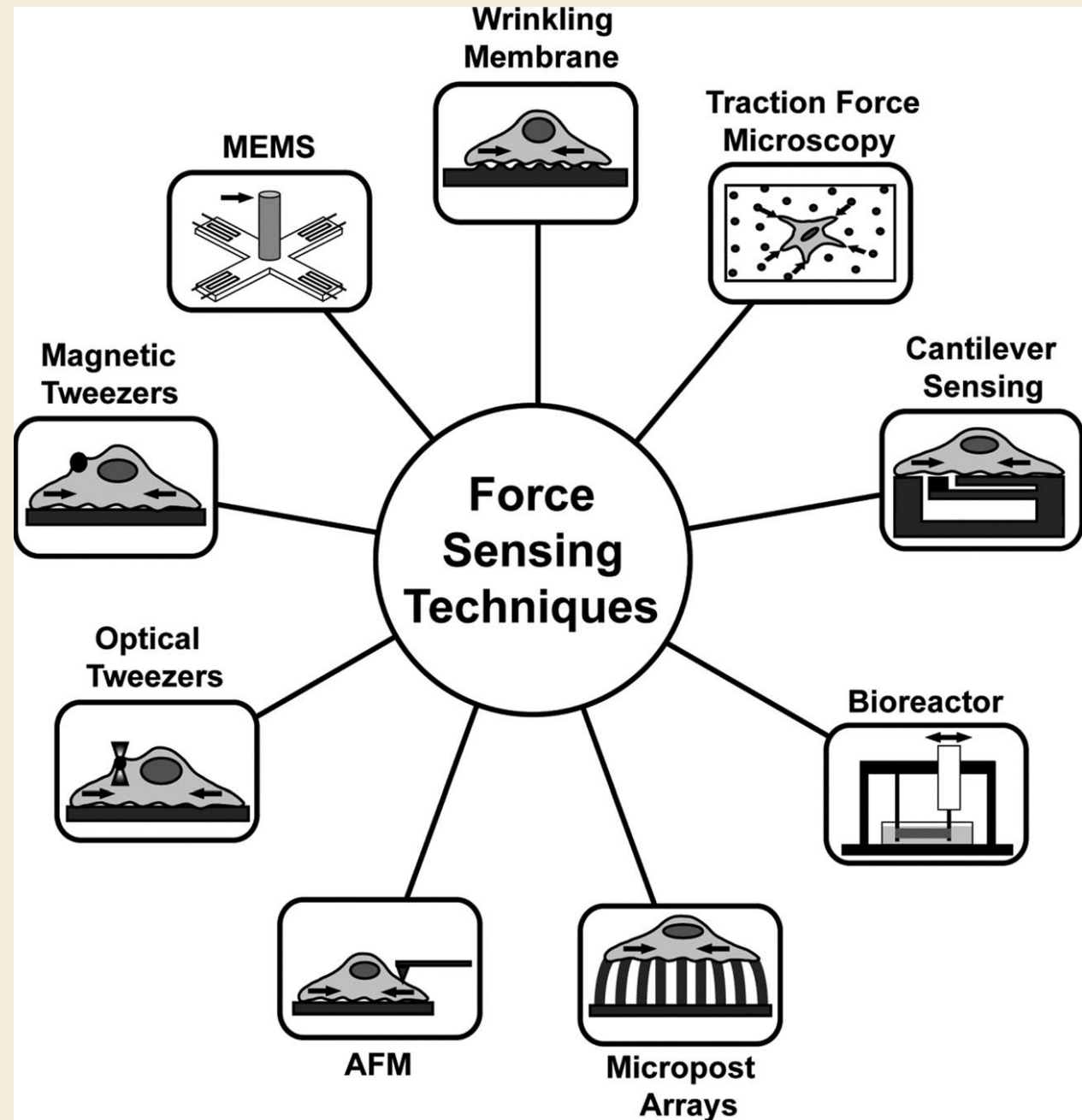
- 4.1. Cellular mechanotransduction (basic principles and examples) L11
- 4.2. Optical, **magnetic and acoustic tweezers** L7, L12
- 4.3. **Super resolution optical microscopy techniques (STED, PALM)** L12

- Lab visit and experimental optical tweezers cell mechanics session at CNR IOM

Force Application Techniques



Force Sensing Techniques



Outline:

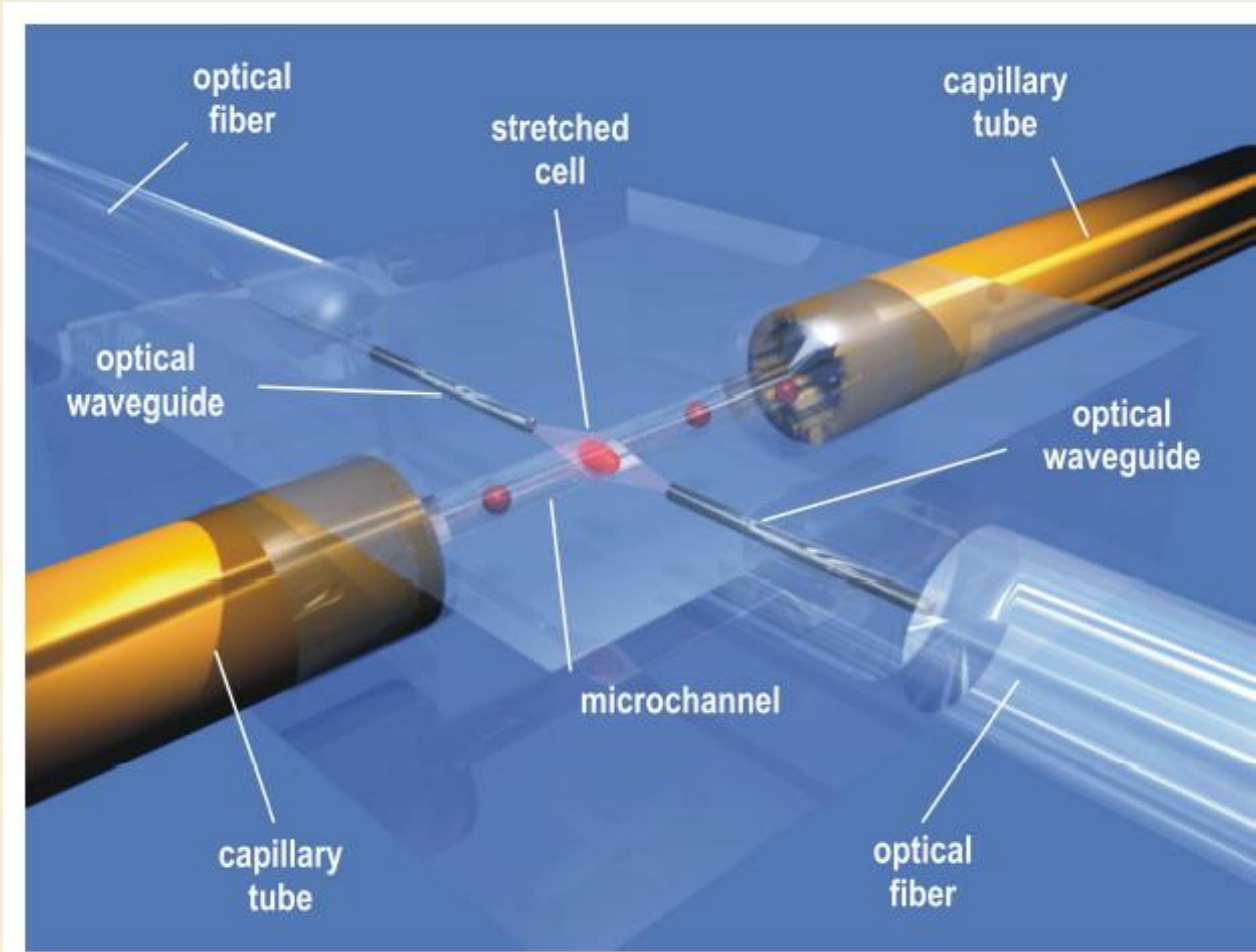
- Optical, stretcher
- Magnetic and acoustic tweezers
- Super resolution optical microscopy techniques (STED, PALM)

? Lab visit and experimental optical tweezers cell mechanics session at CNR IOM

Progress in science depends on new techniques, new discoveries and new ideas, probably in that order.

*Sydney Brenner,
Nobel Prize in Physiology or Medicine 2002*

Cells in suspension are circulated in a fluidic channel and trapped by two counter propagating laser beams.



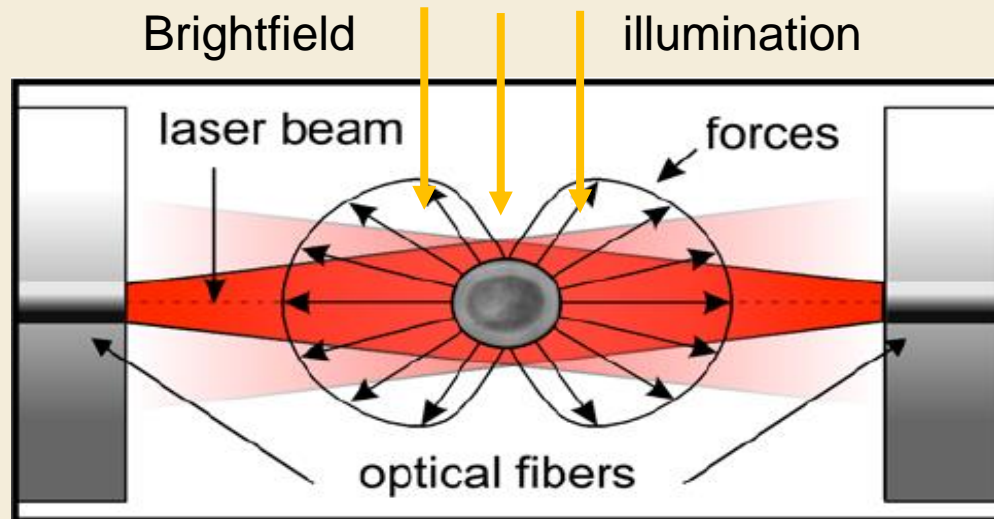
Schematic of the optical stretcher

The laser beams are guided in optical fibers and wave guides integrated lab on chip

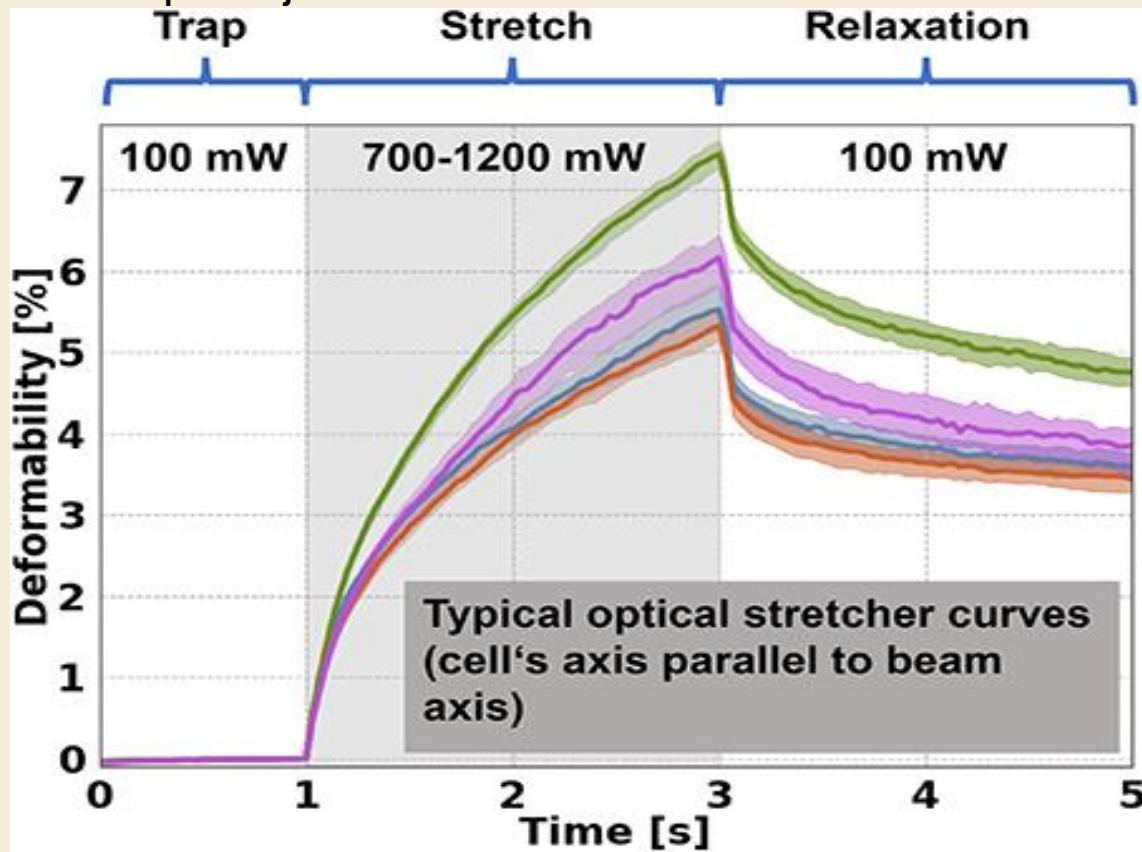
The cells flow through the capillary tubes and micro-channels in a direction orthogonal to the laser beams.

Once a cell is intercepted by the laser beams, it is stopped and stretched by the counterpropagating laser beams exiting the waveguides and coupling into the microchannel.

After stretching the cell is released switching off the lasers. Throughput max: about 2000 cells / h



Microscope obj



Principle of cell stretching

Each laser beam exerts radiation pressure on the opposite wall of the cell, inducing cell stretching.

Power 100 - 1200 mW.

The strain vs time, $\epsilon(t)$, is measured by image processing:

$$\epsilon(t) = a \cdot [1 - \exp(-\lambda t)]$$

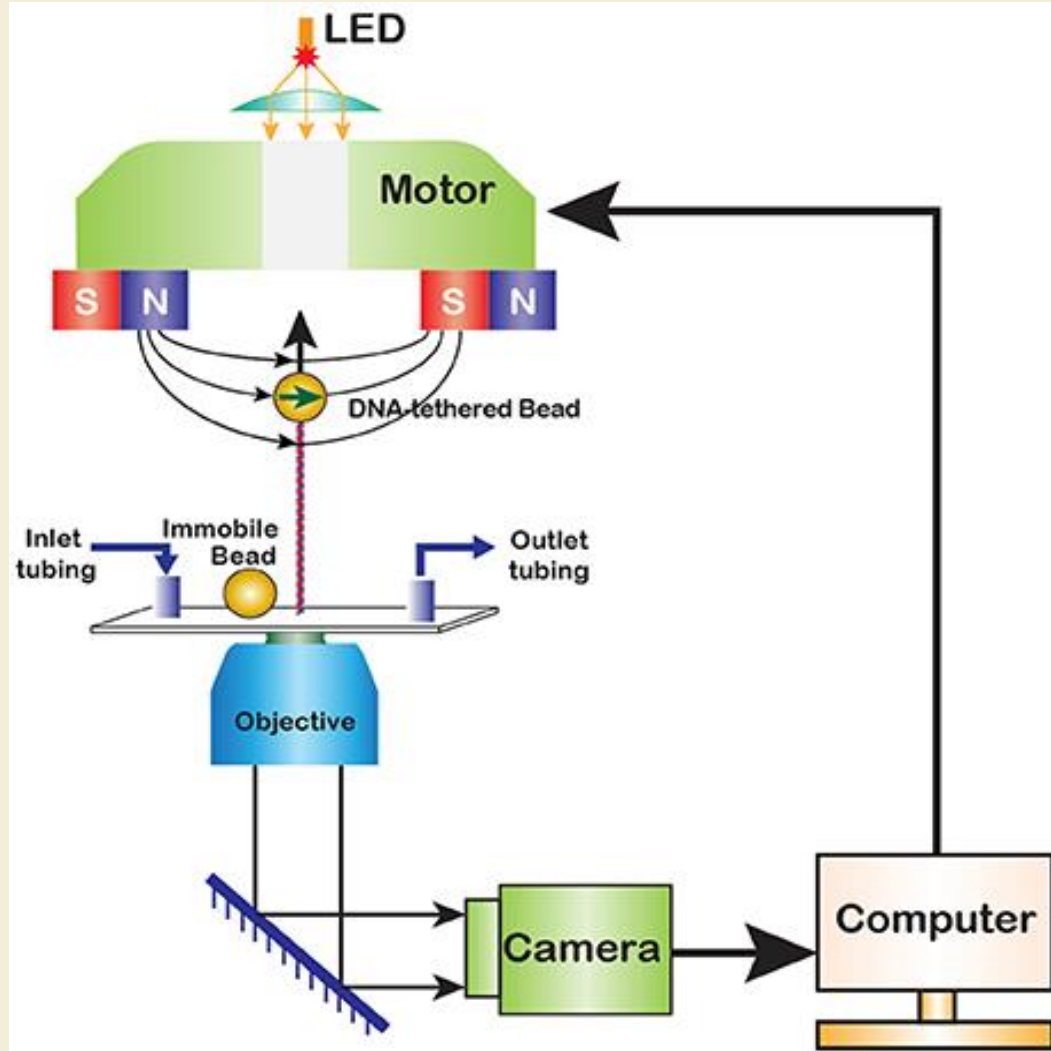
$\lambda = E/\eta$ – characteristic deformation rate

$a = \sigma/E$ - relative amplitude of the stretch

E – elastic constant, η - viscosity constant,

σ – instantaneous constant stress.

The first magnetic tweezers were assembled in 1996 by Strick et al who used them to explore elasticity of supercoiled DNA

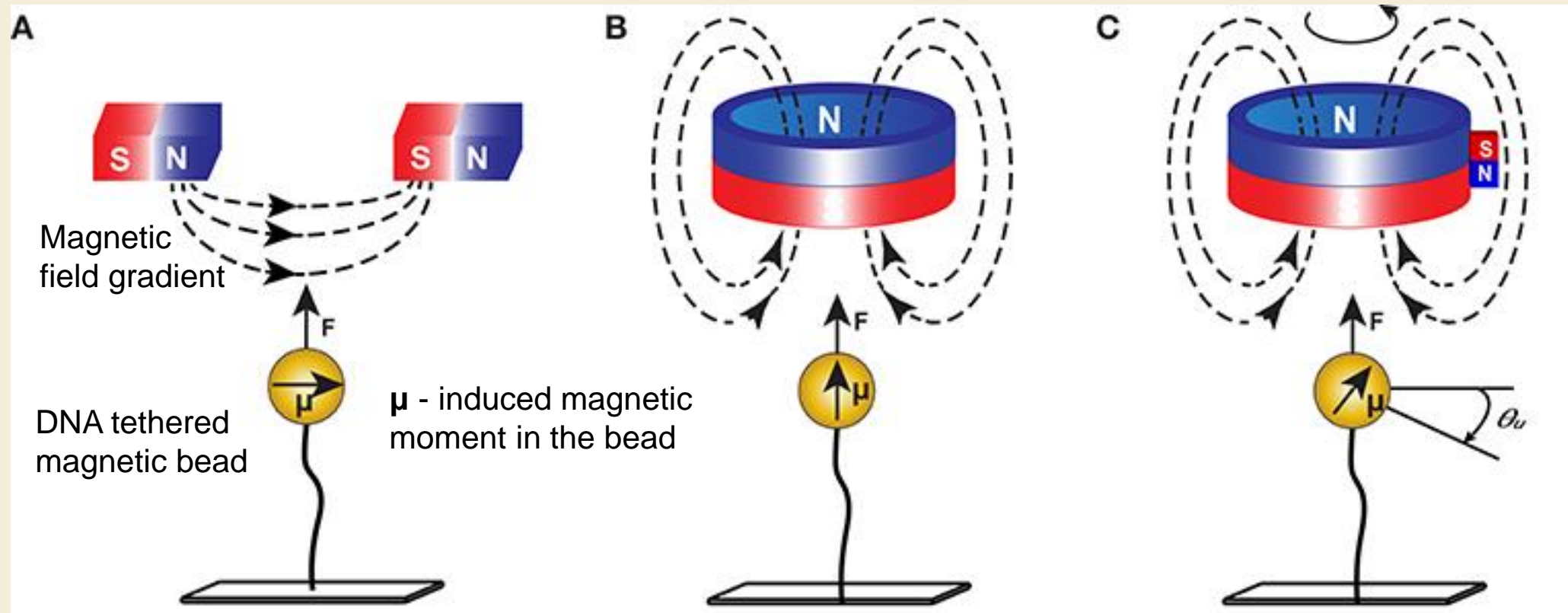


Schematic of magnetic tweezers setup

A paramagnetic bead (e.g. FeO) is tethered to the surface of a flow cell via a functionalized DNA molecule.

Permanent magnets produce magnetic field that pulls the bead in the direction of the field gradient.

The magnets can be translated or rotated to alter the stretching force or twist the DNA.



(A) A pair of horizontally placed magnets induces a horizontal magnetic moment (μ) in the bead. Vertical translation of the magnets induces translation of the bead. Rotation of the magnets around the tether axes induces rotation of the bead.

(B) Cylindrical magnets exert a vertical magnetic field to the tether axis.

(C) Magnetic torque tweezers: a small horizontal field gradient in addition to a strong vertical one.

The force F experienced by the bead in MT:

$$\vec{F} = \frac{V_b \chi}{\mu_0} \nabla |\vec{B}|^2$$

$$\vec{B} = \mu_0 (1 + \chi) \vec{H}$$

\vec{B} – the magnetic flux density (magnetic induction) [T] = [N/Am]

V_b - the bead volume [m³]

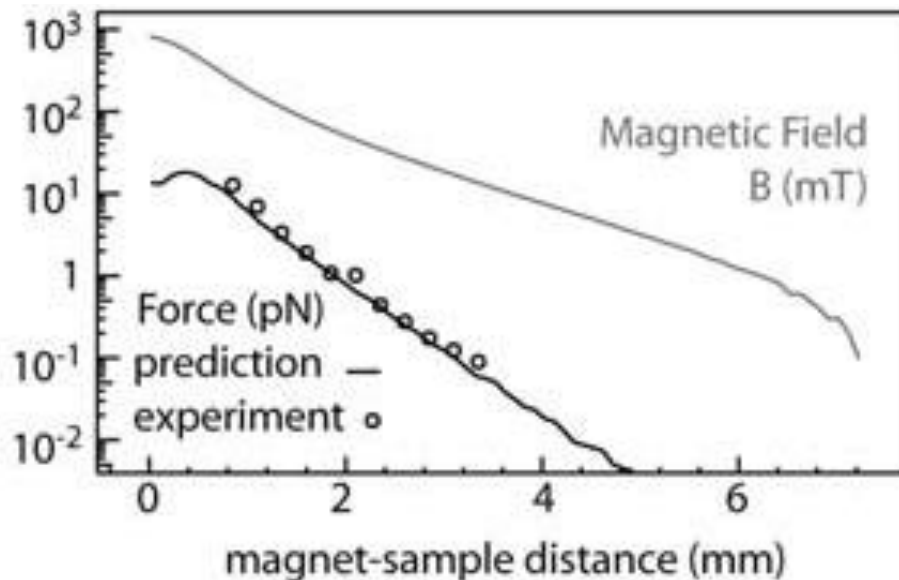
μ_0 - permeability of free space $1.26 \cdot 10^{-6}$ [H/m]=[T m/A]

χ - magnetic susceptibility of the bead (material) [-]

The force F is a function of

- the gradient of the magnetic field
- the volume of the particle (bead)
- the material (paramagnetic $\chi > 0$, superparamagnetic and ferromagnetic $\chi \gg 0$)

Force vs magnet – sample distance



Ex. Using NdFeB (Neodymium Iron Boron) magnets and micrometric beads (2.5 μ m), the MT can produce forces F of 10-20 pN at a distance of about 1 mm, which is sufficient for most of single molecule applications.

The force experienced by a magnetic bead in MT has an expression similar to the gradient force experienced by a dielectric bead in OT :

Magnetic Tweezers MT

$$\vec{m} = V\chi\vec{H} = \frac{V\chi}{\mu_0}\vec{B}$$

$$U = -\vec{m} \cdot \vec{B}$$

$$\vec{F} = -\nabla U = \frac{V\chi}{\mu_0}\nabla|\vec{B}|^2$$

Induced dipole moment

The interaction dipole moment – field (H or E) creates a **potential**:

For a varying field the **force** is:

Optical Tweezers OT

$$\vec{p} = \alpha\vec{E} = 4\pi\epsilon_0V\vec{E}$$

$$U = -\vec{p} \cdot \vec{E}$$

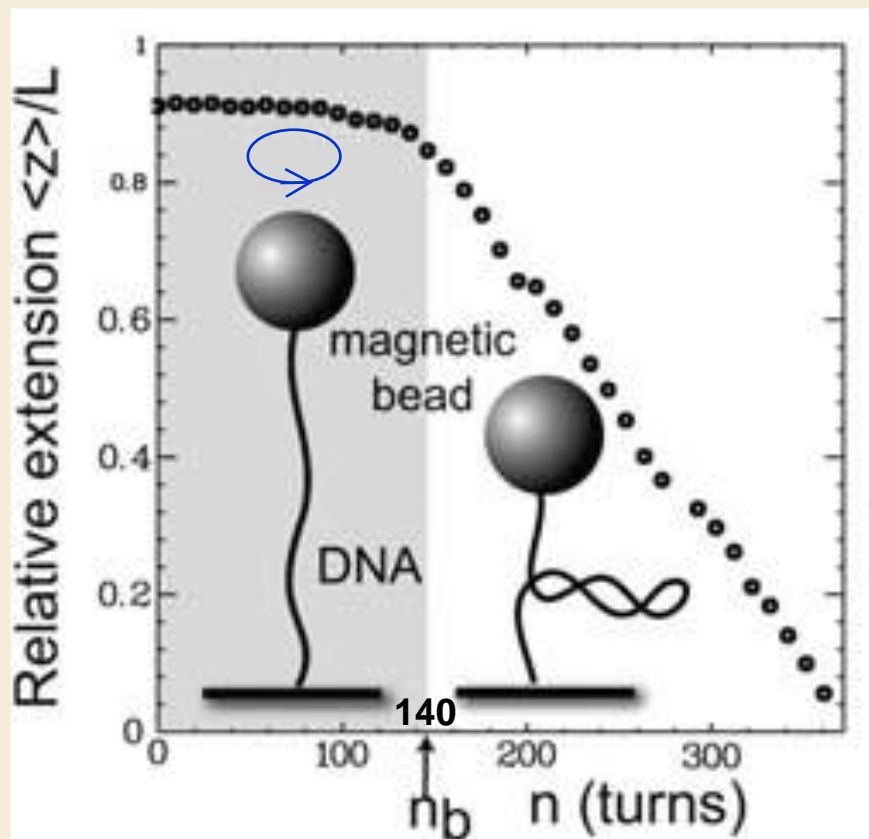
$$\vec{F} = -\nabla U = 4\pi\epsilon_0V\nabla|\vec{E}|^2$$

MT characteristics

- The force due to a magnetic field is analogous to the optical gradient force, with a potential energy due to the response of the particle to an external field.
- MT allows creating an uniform force over a large area, thus enabling many systems to be probed at once → **increase the throughput**.
- The orientation of the field can also be manipulated independent of the gradient, permitting **controlled rotation**, attractive for studying phenomena such as DNA supercoiling.

Twisting DNA with MT

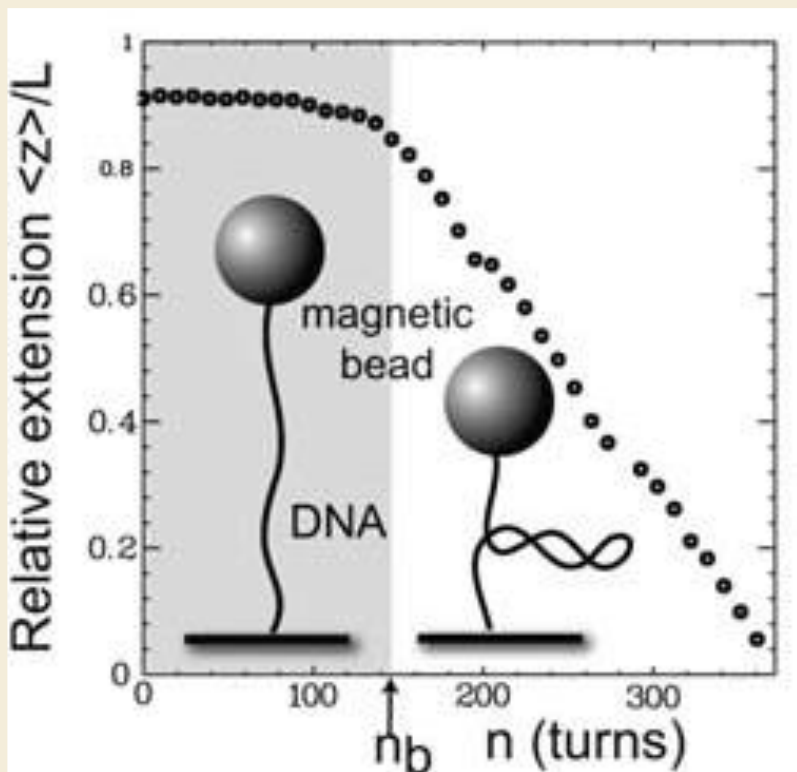
The ease with which DNA can be twisted in a MT setup by rotating the magnets makes this system an optimum choice for the study of coiled (and braided) DNA and its interactions with proteins (e.g., topoisomerases).



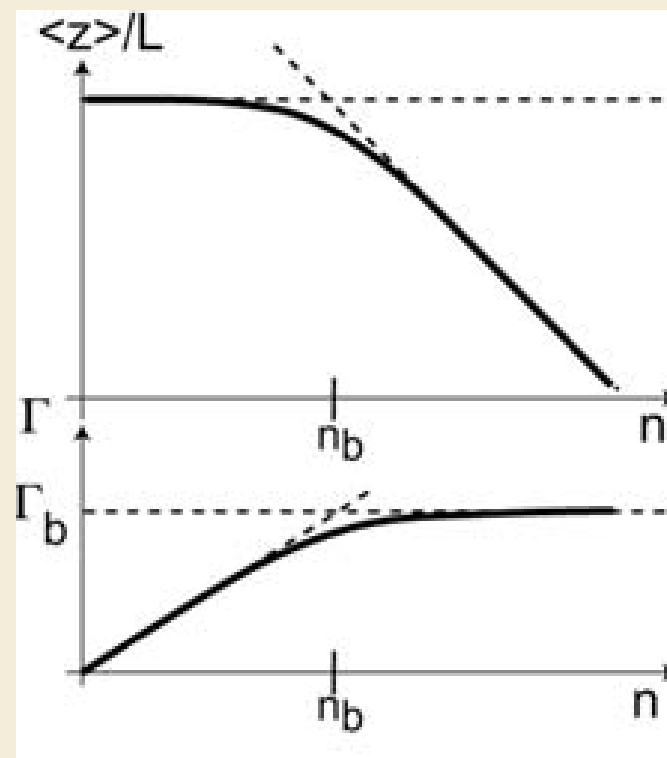
Experimental curve (normalized extension) of one single dsDNA molecule (50 Kb) at $F = 1.2$ pN. At low number of turns n , the change in DNA extension is small, \rightarrow the molecule stores torsional energy.

After $n = n_b \approx 140$, the molecule buckles and starts forming plectonemes. The extension decreases almost linearly.

Extension vs. supercoiling for one dsDNA



A)

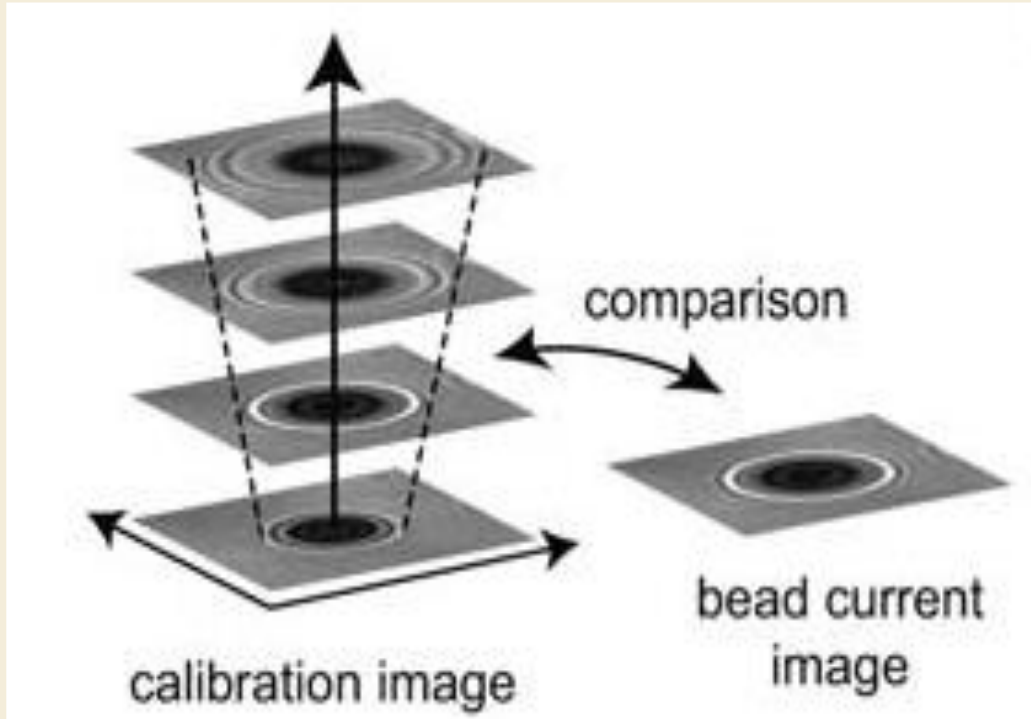


B)

Initial twisting does not change the system's extension, but the torque stored in the tube increases linearly with the number of turns n applied. At $n = n_b$, forming a loop (plectonemes) costs less energy than increasing the torsional energy.

Each additional turn leads to the formation of another loop, so that the extension decreases linearly with n , but the torque $\Gamma = \Gamma_b$ remains constant.

Measurement principle of the bead position in z



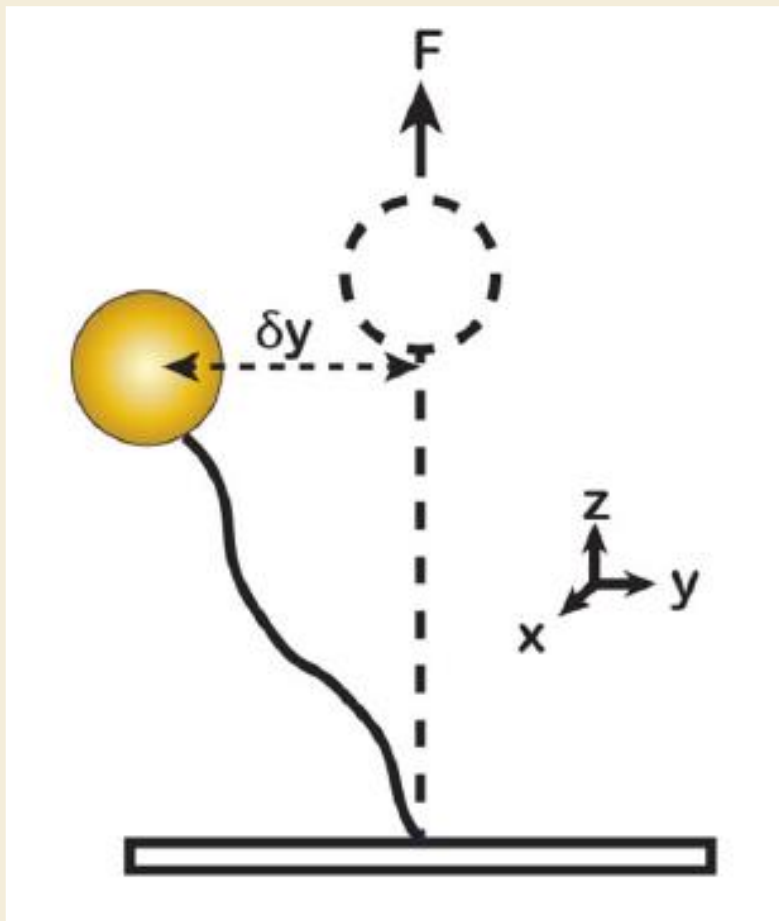
Due to diffraction the bead image is formed by a series of diffraction rings whose sizes depend on the relative distance between the bead and the focal plane. When the bead is in focus, the rings disappear, but they increase in diameter as the bead moves out of focus.

By precisely stepping the focal plane through a series of positions (e.g., by moving the objective with a piezo-electric device), one forms a stack of calibration images that records the shape of the diffraction rings versus distance from the focal plane.

The out-of-focus distance for a new bead image is determined by comparing its diffraction pattern to the calibration stack.

Bead magnetization varies from one bead to another → calibration using Brownian motion is necessary for each bead

Brownian motion of a DNA tethered magnetic bead in solution.



The tethered bead behaves as a harmonic pendulum with the lateral stiffness:

$$k_y = F / l.$$

The stiffness can be calculated from the horizontal fluctuation $\langle \delta y^2 \rangle$ of the bead:

$$k_y = kT / \langle \delta y^2 \rangle$$

or in the frequency domain using the PSD (Power Spectrum Density), in a similar way to Optical Tweezers.

Acoustic tweezers spatially and temporally manipulate matter by using the interaction of sound waves with fluid and solid particle.

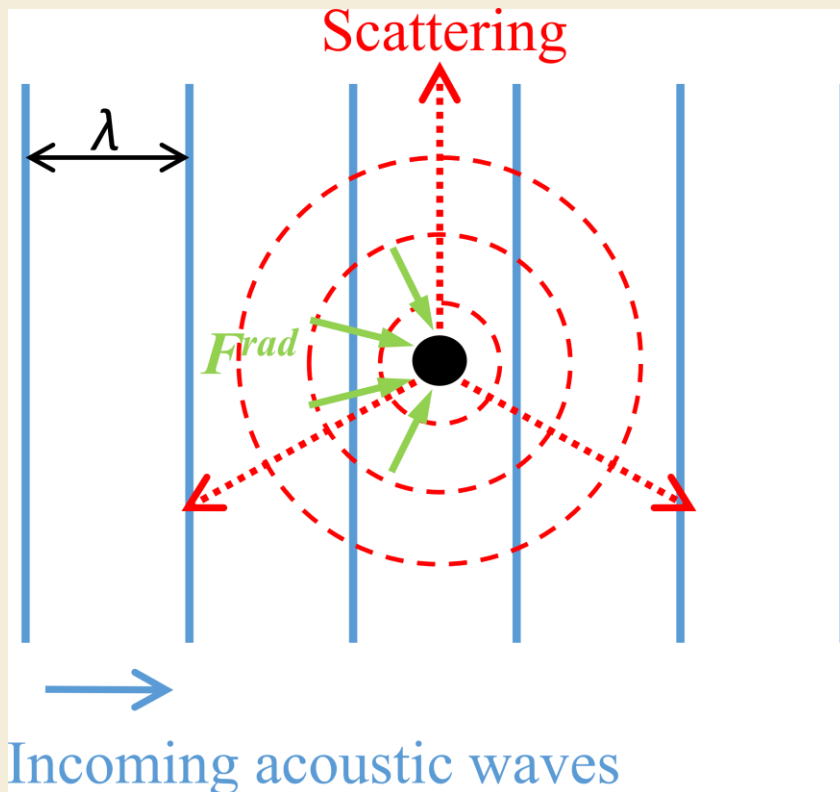
There are three types of acoustic tweezers:

traveling-wave, standing-wave, and acoustic-streaming tweezers.

Both standing-wave and traveling-wave tweezers manipulate particles directly via an applied **acoustic radiation force**, whereas acoustic-streaming tweezers indirectly manipulate particles via **acoustically induced fluid flows**.

A. Ozcelik et al, Acoustic tweezers for life sciences, *Nature Methods* (2018) **15**: 1021.

G. Sitters et al, Acoustic Force Spectroscopy, *Nature Methods* (2014) **12**: 47.



Sketch of the far-field region $r \gg \lambda$ of an incoming acoustic wave ϕ_{in} (vertical lines) of wavelength λ scattering off a small particle (black dot) with radius $a \ll \lambda$, leading to the outgoing scattered wave ϕ_{sc} (circles and arrows).

The radiation force on the particle placed in a standing wave is a gradient force of the form:

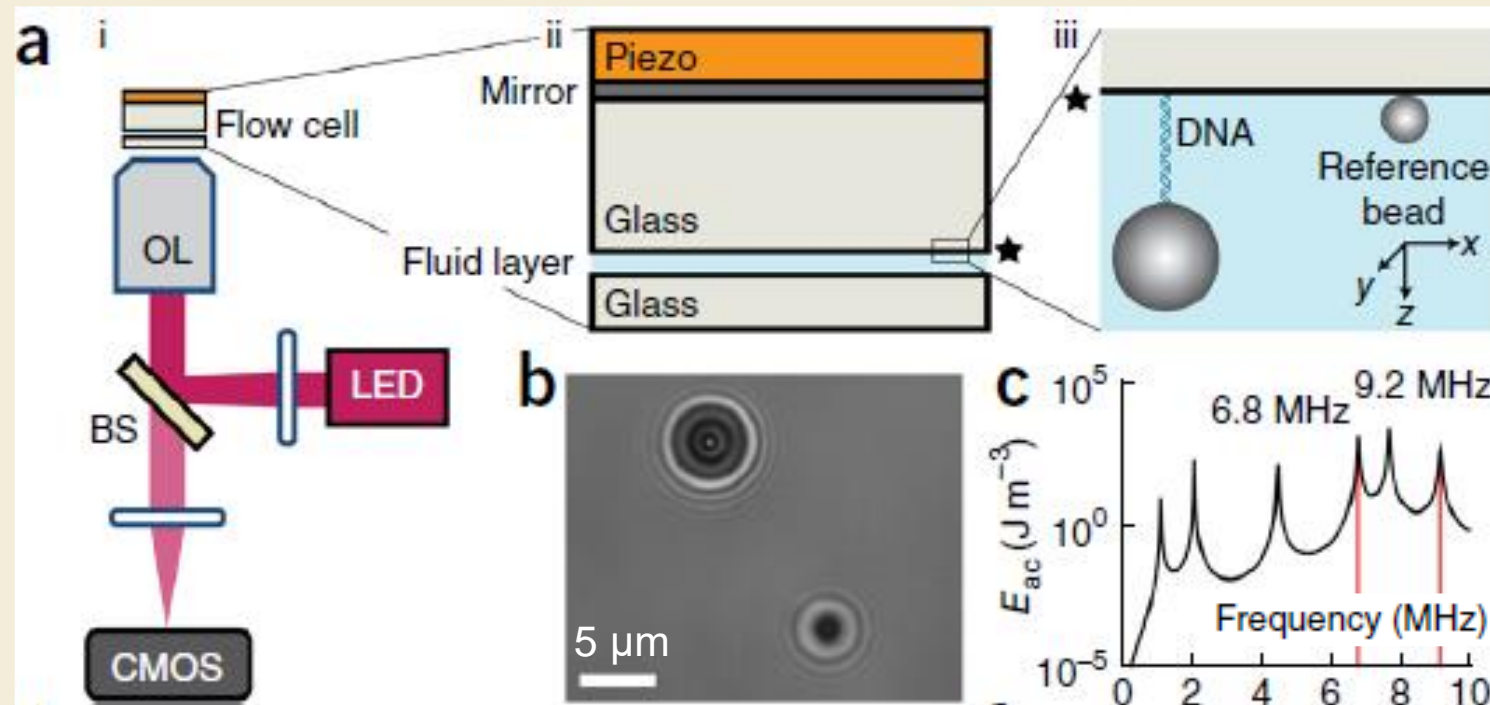
$$\mathbf{F}^{rad} = -\nabla U$$

U - acoustic potential energy
 V - microbead volume

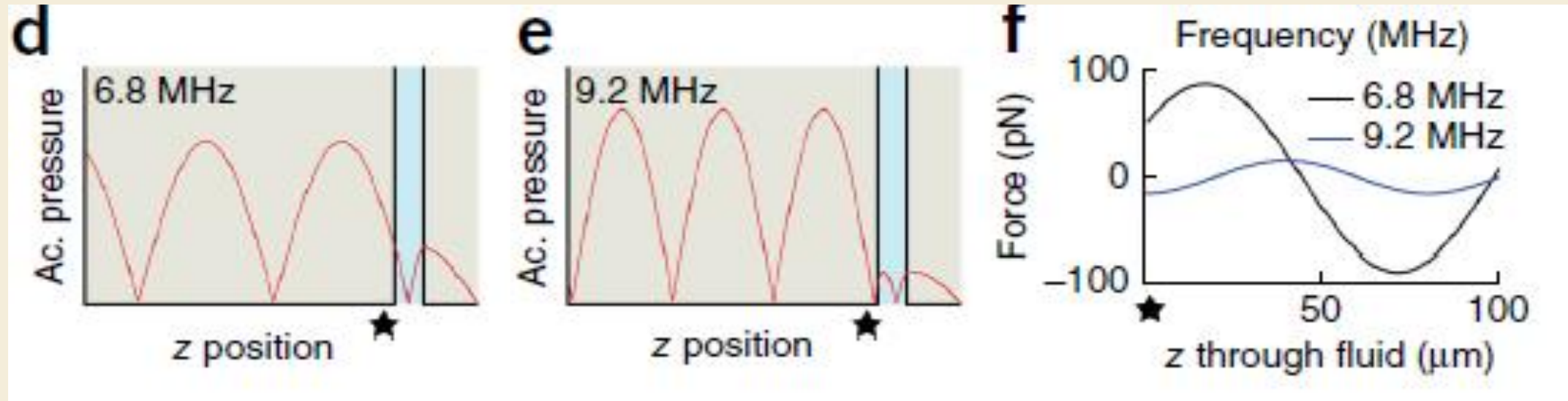
$$F = -V \nabla \left[\frac{1 - \kappa^*}{4} \kappa_m p^2 - \frac{(\rho^* - 1)}{2\rho^* + 1} \rho_m v^2 \right]$$

in which p is the acoustic pressure, v the acoustic velocity, and $\rho^* (= \rho_p / \rho_m)$ and $\kappa^* (= \kappa_p / \kappa_m)$ are the density ratio and compressibility ratio between the particle and the medium, respectively¹¹. In the case of polystyrene or silica microspheres in water, the force is dominated by the gradient of the squared acoustic pressure, driving the microspheres toward an acoustic pressure node.

Acoustic Force Spectroscopy Setup



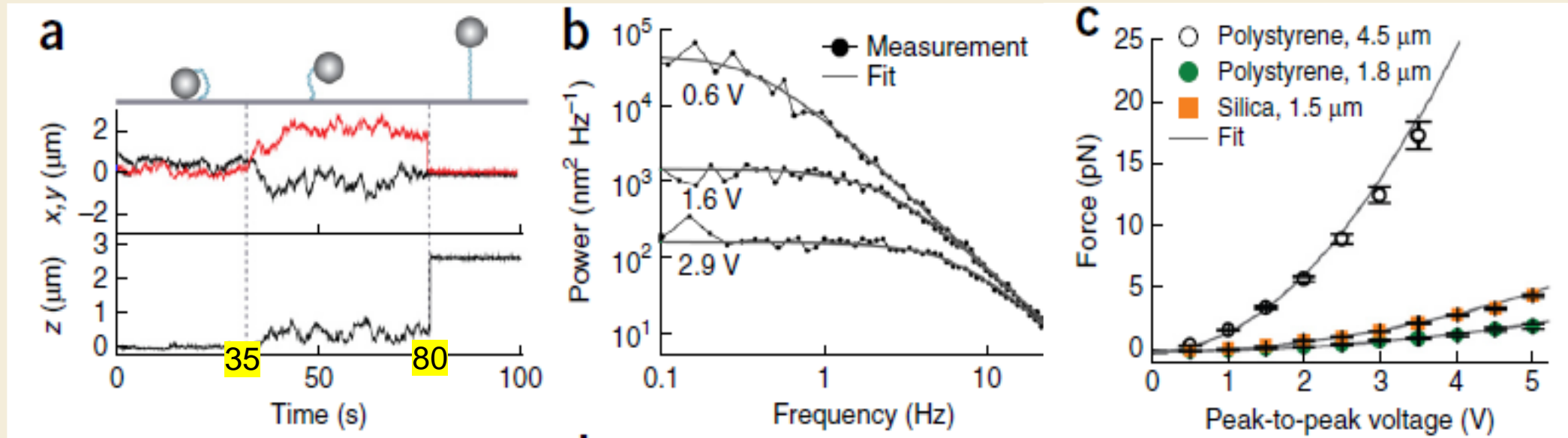
- (a, i) Acoustic force device integrated in a flow cell; objective lens (OL); digital camera CMOS, LED light source.
- (a, ii) Flow cell: two glass plates with a fluid chamber in between. An acoustic wave-generating piezo plate is attached to the upper glass slide, which has a sputtered mirroring aluminum layer for illumination.
- (a, iii) A single DNA molecule, attached at one end to the upper glass plate (black stars) and at the other to a microsphere, is stretched by acoustic forces acting on the microsphere.
- (b) Digital camera image of a DNA-tethered polystyrene microsphere (4.5- μm diameter; DNA length, 8.4 kbp) and a silica reference microsphere (1.5- μm diameter).
- (c) Theoretical acoustic energy (E_{ac}) of the AFS device driven with a peak-to-peak voltage (V_{pp}) of 5 V.



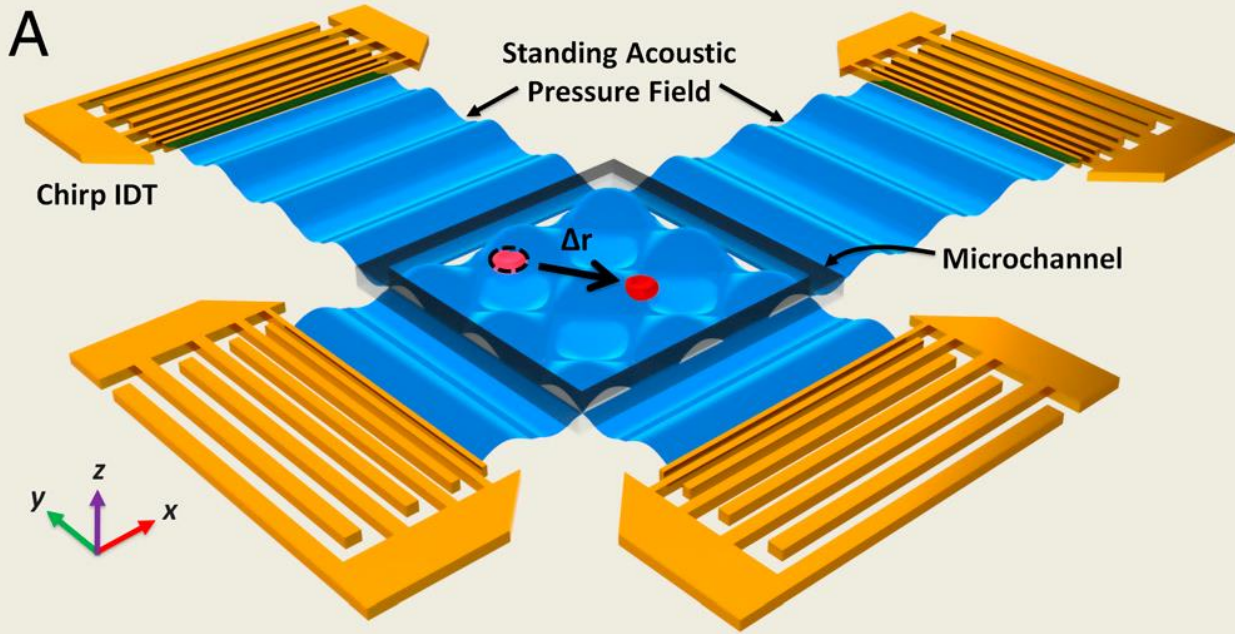
(d,e) Predicted acoustic (Ac.) pressure distribution at 6.8-MHz (d) and 9.2-MHz (e) resonance frequencies across the glass and fluid layers.

(f) Predicted forces for a 4.5- μm -diameter polystyrene microsphere directed along the z direction (0.5-W input power). Microspheres near the upper surface ($z = 0$) experience a force directed away from the surface at 6.8-MHz resonance and toward the surface at 9.2 MHz.

AFS applied to tethered DNA.



- (a) Time traces, x (black) and y (red) position, of a DNA-tethered microsphere (polystyrene, diameter, 4.5 μm ; DNA length, 8.4 kbp). 0- 35 s: piezo driven at 9.0 MHz (peak-to-peak voltage (V_{pp}) = 0.5 V), pushing the microsphere toward the surface. 35–80 s: no acoustic force was applied; > 80 s the piezo was driven at 6.7 MHz (V_{pp} = 2.4 V), pulling the microsphere away from the surface.
- (b) Mean power-spectra values of the microsphere's x position using a Lorentzian function. Forces obtained were 0.61, 3.9 and 11.8 pN at V_{pp} = 0.6, 1.6 and 2.9 V piezo-driving voltages, respectively.
- (c) Forces acting on polystyrene and silica microspheres tethered to the glass surface with DNA (length, 8.4 kbp) as determined from power-spectrum analysis.



Device structure and working mechanism of the SAW

(A) Schematic illustrating a microfluidic device with orthogonal pairs of chirped IDTs for generating standing SAW.

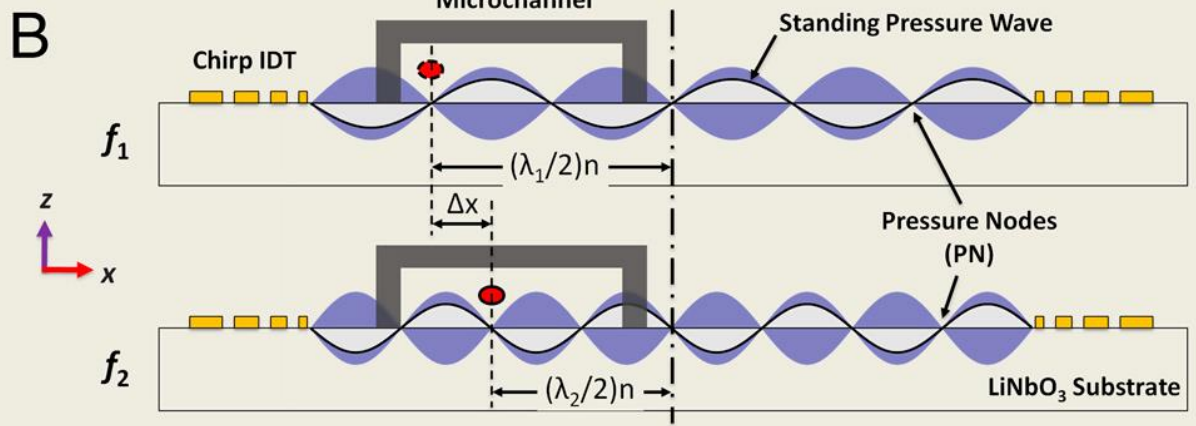
(B) A standing SAW field generated by driving chirped IDTs at frequency f_1 and f_2 . When particles are trapped at the n_{th} pressure node, they can be translated a distance Δx :

$$\Delta x = n (\Delta \lambda / 2) = n(c/f_1 - c/f_2)/2$$

by switching from f_1 to f_2 .

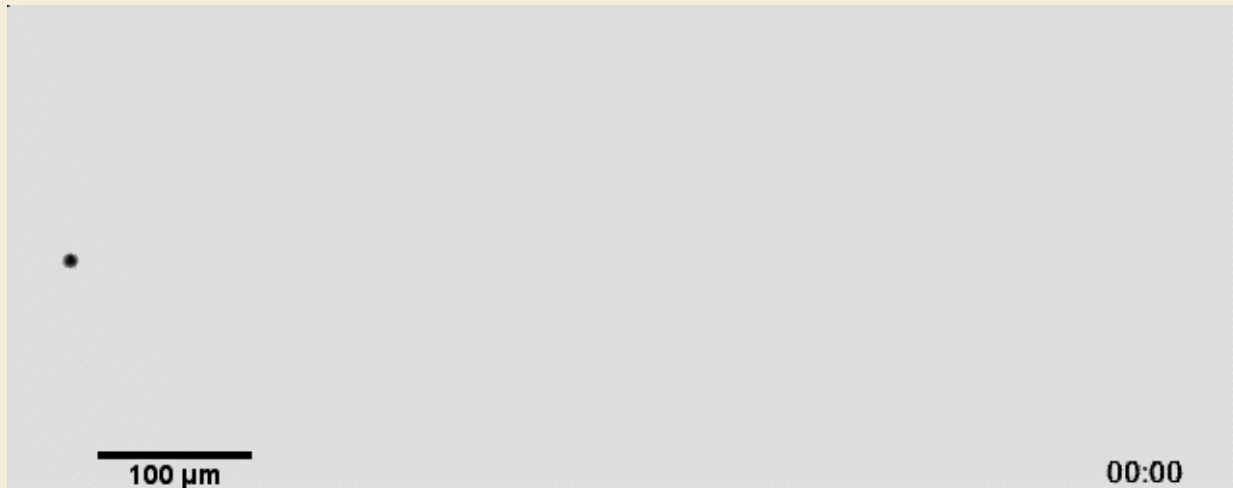
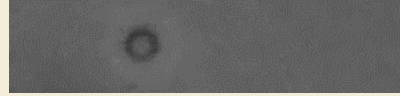
This relationship indicates that the particle displacement can be tuned by varying the pressure node where the particle is trapped.

IDT – Inter Digital Transducer

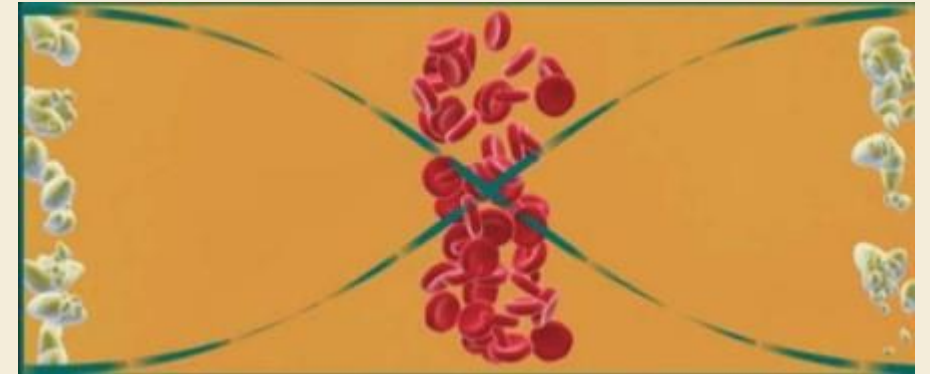


Single particle manipulation in 2D, by SAW.

10 um polystyrene bead.



Separation of lipid particles
(formed by triglycerides leaking from cells)
from erythrocytes



Anti - Node

Node